Journal of Medicinal Chemistry

Article

pubs.acs.org/jmc

Synthesis and Biological Activity of 6-Substituted Pyrrolo[2,3-*d*]pyrimidine Thienoyl Regioisomers as Inhibitors of de Novo Purine Biosynthesis with Selectivity for Cellular Uptake by High Affinity Folate Receptors and the Proton-Coupled Folate Transporter over the Reduced Folate Carrier

Lei Wang,[†,#] Christina Cherian,[‡,∥,#] Sita Kugel Desmoulin,[§,∥] Shermaine Mitchell-Ryan,[§] Zhanjun Hou,[‡,∥] Larry H. Matherly,*[,§,∥,⊥,‡,#] and Aleem Gangjee*[,†,#]

[†]Division of Medicinal Chemistry, Graduate School of Pharmaceutical Sciences, Duquesne University, 600 Forbes Avenue, Pittsburgh, Pennsylvania 15282, United States

[‡]Developmental Therapeutics Program, Barbara Ann Karmanos Cancer Institute, 110 East Warren Avenue, Detroit, Michigan 48201, United States

[§]Cancer Biology Graduate Program, [∥]Department of Oncology, and [⊥]Department of Pharmacology, Wayne State University School of Medicine, Detroit, Michigan 48201, United States

Supporting Information

ABSTRACT: We previously reported the selective transport of classical 2-amino-4-oxo-6-substituted pyrrolo[2,3-*d*]pyrimidines with a thienoyl-for-benzoyl-substituted side chain and a three- (**3a**) and four-carbon (**3b**) bridge. Compound **3a** was more potent than **3b** against tumor cells. While **3b** was completely selective for transport by folate receptors (FRs) and the proton-coupled folate transporter (PCFT) over the reduced folate carrier (RFC), **3a** was not. To determine if decreasing the distance between the bicyclic scaffold and L-glutamate in **3b** would preserve transport selectivity and potency against human tumor cells, **3b** regioisomers with [1,3] (**7** and **8**) and [1,2] (**4**, **5**, and **6**) substitutions on the thienoyl ring and with acetylenic insertions in the four-atom bridge were synthesized and evaluated. Compounds **7** and **8** were potent nanomolar inhibitors of KB and IGROV1 human tumor cells with complete selectivity for FRα and PCFT over RFC.

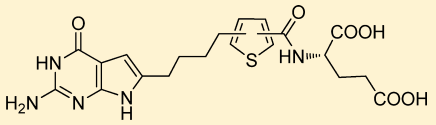

INTRODUCTION

Membrane transport of antifolate therapeutics such as methotrexate MTX is integral to chemotherapy efficacy in treating a variety of malignancies and nonmalignant diseases.[1] The major membrane transporters include the reduced folate carrier (RFC), the proton-coupled folate transporter (PCFT), and the high affinity folate receptors (FRs) α and β.[1−4] While all systems transport folate cofactors and classical antifolates such as MTX, raltitrexed (RTX), and pemetrexed (PMX), they differ in terms of mechanism and substrate specificities. Whereas both RFC and PCFT are integral membrane proteins that act as facilitative transporters, FRs are glycosyl phosphatidylinositol-modified proteins that mediate cellular uptake of (anti)folates by receptor-mediated endocytosis.

The major folate transporters also differ in terms of their tissue distributions. For instance, RFC is ubiquitously expressed in tumors and tissues and is the primary uptake mechanism for folate cofactors.[1] FRs are expressed abundantly in certain malignancies, most notably as the FRα isoform in ovarian carcinomas, and in a limited number of normal epithelial tissues such as renal tubules.[2] Major sites of PCFT expression include the upper small intestine (e.g., jejunum) and the liver and kidney.[3,5,6] In solid tumors such as hepatomas, ovarian carcinomas, and non-small-cell lung carcinomas, PCFT is highly expressed.[7] PCFT exhibits an acidic pH optimum,[4,6] which is compatible with the low pH microenvironments of the small intestine and many solid tumors. While PCFT is modestly expressed in most other normal tissues, for those in which PCFT is expressed they are unlikely to present the low pH conditions optimal for membrane transport by this mechanism.[3]

Membrane transport of classical antifolates by RFC in itself would likely result in limited drug selectivity toward tumors over normal proliferative tissues such as bone marrow, since these normal tissues all express RFC. The concept of selectively targeting FR-expressing tumors with folate-based antitumor agents has been tested. Examples of folate-based therapeutics include **1** [(2*R*)-2-((4*R*)-4-carboxy-5-(4-((2-(hydroxymethyl)-4-oxo-4,6,7,8-tetrahydro-3*H*-cyclopenta[*g*]quinazolin-6-yl)(prop-2-yn-1-yl)amino)phenyl)-5-oxopentanamido)pentanedioic acid] [ONX0801 (BGC945)], a small molecule antifolate licensed by Onyx Pharmaceuticals which is selectively transported by FRs and inhibits thymidylate synthase,[8] and vincaleukoblastin-23-oic acid, O4-deacetyl-, 2-[(2-mercaptoethoxy)carbonyl]hydrazide,

Received: December 14, 2011
Published: January 13, 2012

dx.doi.org/10.1021/jm201688n | *J. Med. Chem.* 2012, 55, 1758−1770

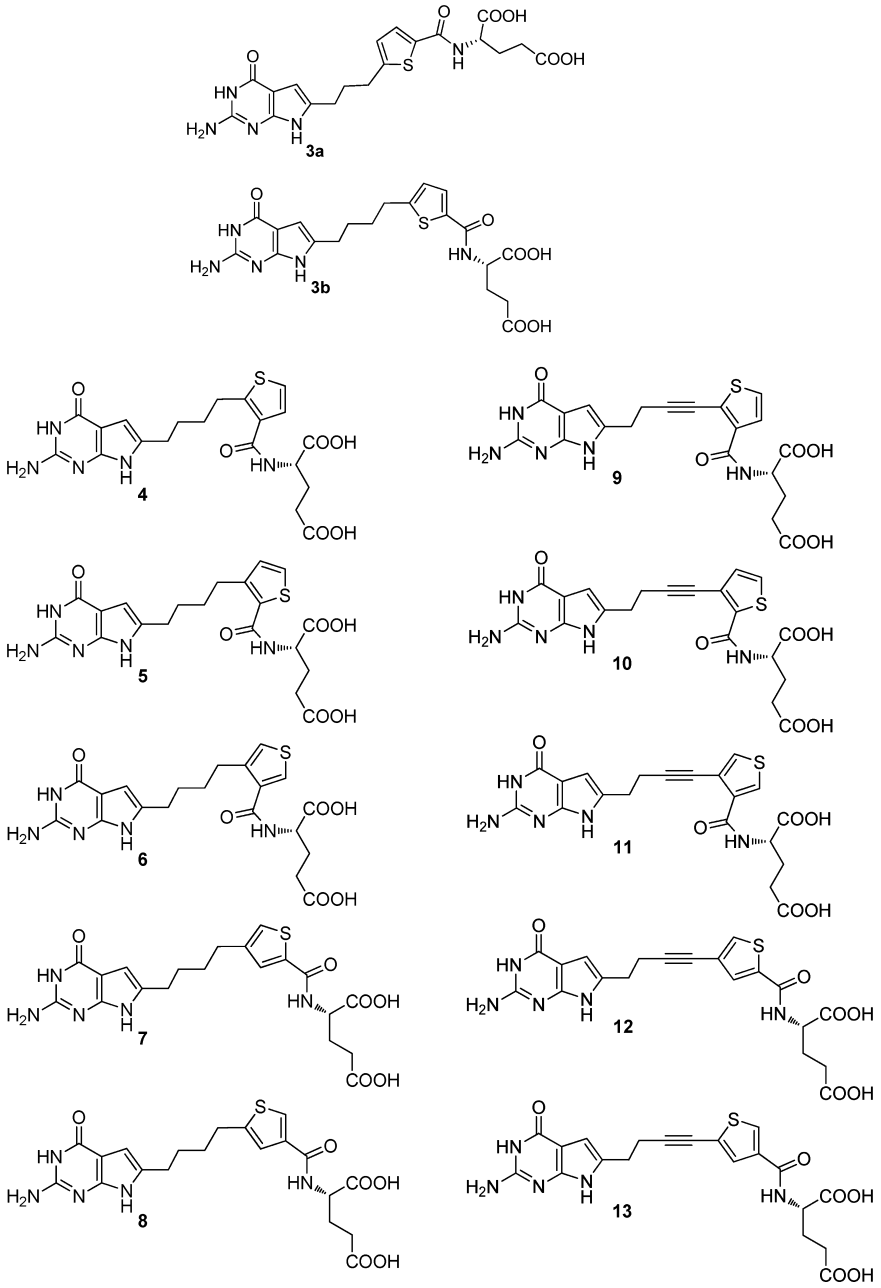

Figure 1. Structures of 6-substituted pyrrolo[2,3-*d*]pyrimidines **3a** and **3b** and the thienoyl regioisomers **4**–**13**.

disulfide with *N*-[4-[[(2-amino-1,4-dihydro-4-oxo-6-pteridinyl)-methyl]amino]benzoyl]-L-*γ*-glutamyl-L-*α*-aspartyl-L-*α*-aspartyl-L-cysteine **2** [EC-145 (Endocyte)], a desacetylvinblastine monohydrazide–folic acid complex.[9] Compound **1** is in clinical trials in the U.K. A randomized phase II trial was performed in which **2** with doxorubicin was compared to doxorubicin alone for the treatment of platinum-resistant ovarian cancer (ClinicalTrials.gov identifier: NCT00722592).

We recently identified 6-substituted pyrrolo- and thieno[2,3-*d*]-pyrimidine antifolates with selective membrane transport by PCFT and/or FRs over RFC, resulting in selective inhibition of proliferation of cells expressing these systems including human tumors.[7,10−14] FR targeting to tumors is based on patterns of expression and basolateral membrane localization unique to tumor cells. In terms of PCFT, the notion of using this transport mechanism to selectively deliver chemotherapy drugs is appealing given the low pH microenvironments of many solid tumors that approximate the pH optimum for PCFT.[15−17] The pyrrolo[2,3-*d*]-pyrimidine thienoyl analogues **3a** and **3b** (Figure 1) with three and four carbons, respectively, in the bridge between the pyrrolo[2,3-*d*]pyrimidine ring and the thiophene ring were the most potent of this series against cells expressing FRs and/or PCFT.[12,13] Cytotoxicity was attributed to the potent inhibition of *β*-glycinamide ribonucleotide (GAR) formyltransferase (GARFTase), which catalyzes the first folate-dependent reaction in de novo purine nucleotide biosynthesis.

Our finding that compound **3a** was more potent than **3b** toward FR- and PCFT-expressing cells suggested that the distance between the bicyclic scaffold and the L-glutamate may be a critical determinant of drug activity.[13] However, in engineered hamster cells, transport selectivity for FR*α* and PCFT over RFC with compound **3a** was less complete than for **3b**. We hypothesized

dx.doi.org/10.1021/jm201688n | *J. Med. Chem.* 2012, 55, 1758−1770

Scheme 1[a]

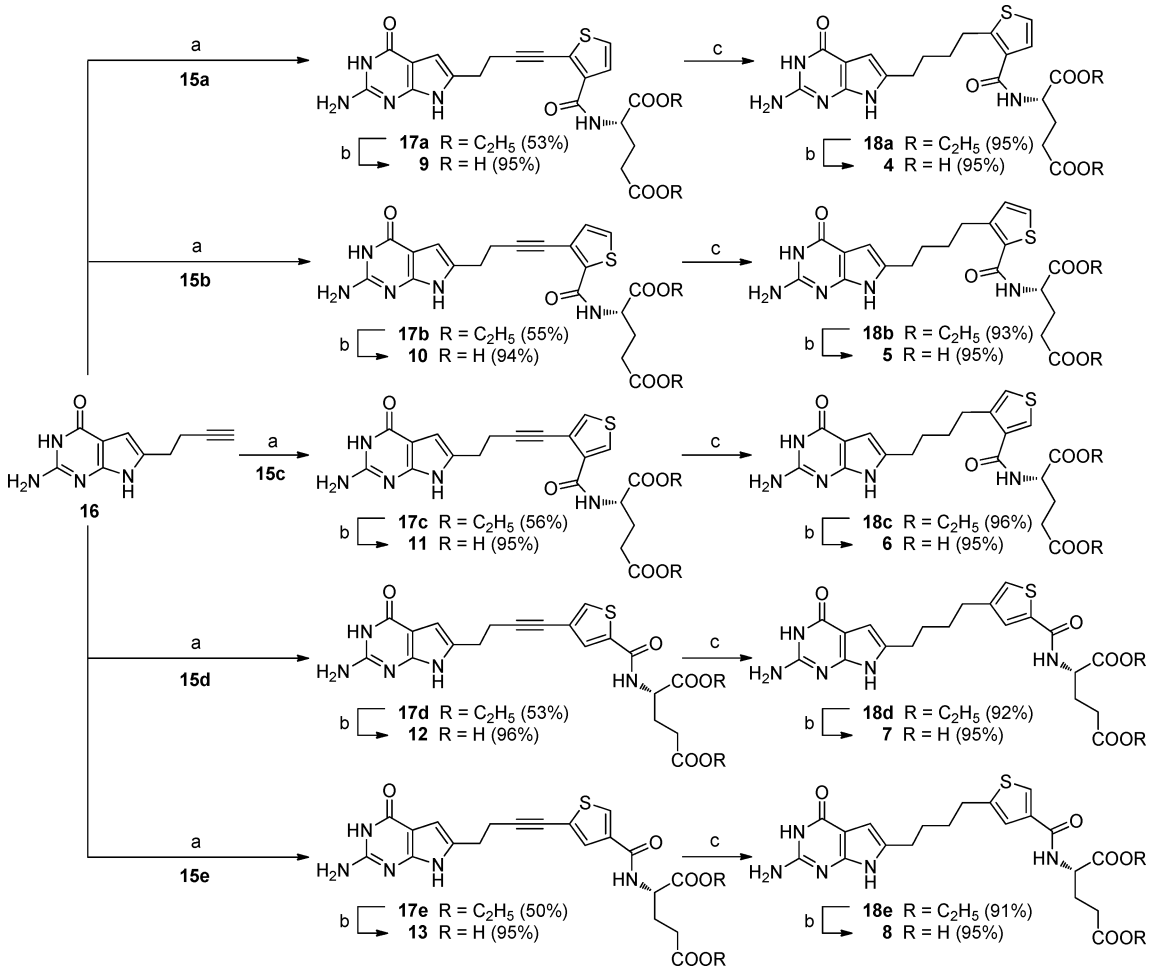

[a]Reagents and conditions: (a) CuI, $Pd(0)(PPh_3)_4$, Et_3N, DMF, room temp, 12 h; (b) (i) 1 N NaOH, MeOH, $CHCl_3$, room temp, 6 h; (ii) 1 N HCl; (c) 10% Pd/C, H_2, 55 psi, 4 h.

that structurally engineered substitutions on the thiophene ring of **3a** would afford distances between the bicyclic scaffold and the L-glutamate midway between those for the three-atom bridge **3a** and the four-atom bridge **3b**. We predicted that this would preserve the potency of **3a** along with the selectivity for FRα and PCFT as in **3b**.

We synthesized **3b** regioisomers, differing in positions of substitution of the four-atom carbon bridge and the L-glutamic acid on the thiophene ring (compounds **4**–**8**) and in the presence of a linear, shorter acetylenic linkage (compounds **9**–**13** and **20**) in the carbon bridge region (Figure 1). These modifications decreased the distances between the bicyclic pyrrolo[2,3-*d*]pyrimidine and the L-glutamate moieties in order to systematically determine their impact on drug selectivity for FRs and PCFT over RFC and on potency against human tumor cells. In this report, we describe the synthesis and biologic properties of compounds **4**–**13** (Figure 1) and **20** (Scheme 3).

CHEMISTRY

The synthesis of target compounds **4**–**8** (Scheme 1) started from the reported intermediate **16**.[12] A Sonogashira coupling of **16** with various bromo-substituted thiophene carboxylates **15a**–**e** (Scheme 2) afforded **17a**–**e** in 50–56% yield. Subsequent hydrogenation and saponification of **17a**–**e** afforded target compounds **4**–**8**. Direct hydrolysis of intermediates **17a**–**e** provided conformationally restricted analogues **9**–**13**. Compounds **15a**–**e** (Scheme 2) required in Scheme 1 were synthesized by a peptide coupling of the commercially available bromo-substituted thiophene carboxylic acids **14a**–**e**

Scheme 2[a]

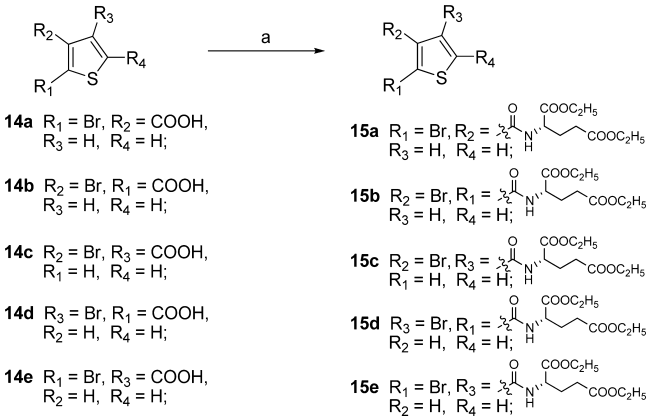

[a]Reagents and conditions: (a) *N*-methylmorpholine, 2-chloro-4,6-dimethoxy-1,3,5-triazine, L-glutamate diethyl ester hydrochloride, DMF, room temp, 12 h.

dx.doi.org/10.1021/jm201688n | *J. Med. Chem.* 2012, 55, 1758–1770

Scheme 3[a]

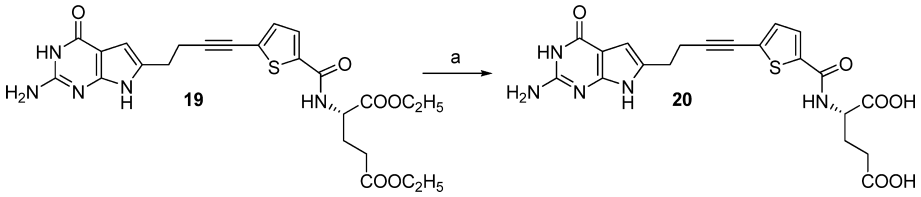

[a]Reagents and conditions: (a) (i) 1 N NaOH; (ii) 1 N HCl.

(Scheme 2) with L-glutamate diethyl ester hydrochloride in 89–91% yield.

Compound **19** (Scheme 3) was previously reported as a precursor to **3b** (Figure 1).[12] For comparison to **3b**, it was also of interest to synthesize and evaluate the classical analogue **20** derived from **19**. Synthesis of **20** from **19** is shown in Scheme 3.

BIOLOGICAL EVALUATION AND DISCUSSION

6-Substituted Pyrrolo[2,3-*d*]pyrimidine Thienoyl Regioisomers as Inhibitors of Cell Proliferation. The distance between the bicyclic scaffold and L-glutamate portions of a series of pyrrolo- and thieno[2,3-*d*]pyrimidine antifolates seems to dictate both selectivity for cellular uptake by FRs and PCFT over RFC and cytotoxic potencies against tumor cells.[10−14] Thus, decreasing the bridge lengths from eight carbons to four carbons was accompanied by substantially increased antiproliferative activities, reflecting transport by PCFT and/or FRs and inhibition of intracellular GARFTase. Decreasing the bridge length from four to three carbons further increased drug potencies. However, for the pyrrolo[2,3-*d*]pyrimidine thienoyl antifolate series, this appeared to be accompanied by some loss of absolute transporter specificity for FRs and/or PCFT over other modes of uptake.[13] Finally, for all series, analogues with bridge lengths less than three carbons showed substantially decreased drug activities.

In the present study, we used the pyrrolo[2,3-*d*]pyrimidine thienoyl platform with a four-carbon bridge. We systematically assessed the effects on cell proliferation for an expanded series of pyrrolo[2,3-*d*]pyrimidine thienoyl regioisomers of **3b** with a four-carbon bridge and thienoyl ring substitutions, 2′,3′ (**4**), 4′,5′ (**5**), 3′,4′ (**6**), 3′,5′ (**7**), and 2′,4′ (**8**) (Figure 1), as an alternative approach for decreasing the distance between the bicyclic pyrrolo[2,3-*d*]pyrimidine and the L-glutamate portions. Hence, in analogues **4**–**6**, the 1,2-substitution pattern on the thiophene forces the bicyclic scaffold and L-glutamate closer together than in the parent four-atom bridge compound **3b** which includes a 1,3-pattern on the thiophene ring. Compounds **7** and **8**, and also 1,3-substitution on the thiophene ring, have an intervening smaller carbon compared to the larger sulfur in **3b**. Further, the C−C−C (112°) bond angle of both **7** and **8** is larger than the C−S−C (91.8°) bond angle of **3b**, and the lengths of the C−S (1.71 Å) and C−C (1.38 Å) bonds are also different (Figure 2, MOE 2008.10).[18] Molecular modeling (Figure 2, MOE 2008.10) shows that the distances from the α-carbon of the bridge to the amide carbonyl are shorter in compounds **7** and **8** (5.10 and 5.11 Å, respectively) than that in **3b** (5.33 Å). The distances from the bicyclic scaffold to the L-glutamate for compounds **7** and **8** are designed to be between those for **3b** and **3a**.

Compounds **9**–**13** and **20** are analogues of **3b**–**8** and contain a single conformational restriction in the four-carbon atom bridge, in the form of a linear acetylenic linkage instead of the saturated C−C linkage of **3b**–**8**. This also provides some

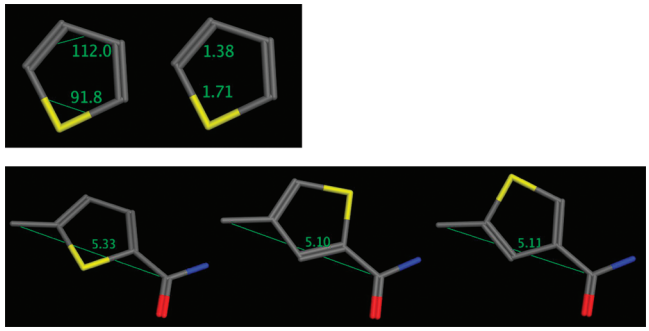

Figure 2. Molecular modeling of the thiophene ring (MOE 2008.10) and angles and distances of the regioisomers of **3b**.

conformational rigidity in the four-carbon atom chain and decreases the length of the carbon bridge (3.52 Å), compared to the saturated analogues (3.87 Å) **3b**–**8**.

Compounds **4**–**13** and **20** were initially screened for growth inhibition in a series of cell lines with defined expression patterns of the major (anti)folate transporters for comparison with compound **3b**. The experimental models were a panel of isogenic Chinese hamster ovary (CHO) sublines derived from RFC-, FR-, and PCFT-null MTXRIIOua^{R}2-4 CHO cells engineered to express FRα (RT16),[10] human RFC (PC43-10),[18] or human PCFT (R2/hPCFT4).[5,11] Additional growth inhibition studies were performed with KB and IGROV1 human tumor cells that express FRα, RFC, and PCFT. We previously showed that during cell outgrowth, the pH of the culture medium decreased from pH 7.2 to ∼6.8 [14] such that all three transporters would be active in drug transport.

For measurements of inhibitory effects on cell proliferation, the cell lines were cultured with the antifolates over a range of concentrations, as described in the Experimental Section. With RT16 CHO, KB, and IGROV1 cells, FRα-mediated drug uptake was established with a parallel culture treated with the cytotoxic drugs and excess (200 nM) folic acid to block FRs. For the PC43-10 and R2/hPCFT4 CHO sublines, results were compared to those for parental R2 cells or to vector-control R2 cells transfected with empty pcDNA3.1 vector [designated R2(VC)]. Patterns of drug sensitivity or resistance for the novel pyrrolo[2,3-*d*]pyrimidine analogues were compared to those for compounds **3a** and **3b** and to those previously reported for classic antifolates (e.g., MTX, PMX, LMTX, RTX).[10−14] Results of the cell proliferation assays are summarized in Table 1.

MTX, PMX, RTX, and LMTX were all active (albeit variably) toward RFC-, PCFT-, or FRα-expressing CHO cells. The 6-substituted pyrrolo[2,3-*d*]pyrimidine thienoyl analogues with *contiguous* thiophene substitutions [2′, 3′ (**4** and **10**), 4′, 5′ (**5** and **11**), 3′, 4′ (**6** and **12**)] were *completely inactive* toward the RFC- and PCFT-expressing CHO sublines. Compounds **7**, **8**, **13**, and **20** were likewise inert toward PC43-10 cells, although

dx.doi.org/10.1021/jm201688n | J. Med. Chem. 2012, 55, 1758−1770

Table 1. IC_{50} (in nM) for 6-Substituted Pyrrolo[2,3-*d*]pyrimidine Thienoyl Regioisomers 3b, 4−13, and 20, Compared to IC_{50} for 3a and Classical Antifolates in RFC, PCFT, and FR-Expressing Cell Lines[a]

	RFC		hFRα		PCFT		RFC/FRα/PCFT		RFC/FRα/PCFT	
antifolate	PC43-10	R2	RT16	RT16 (+FA)	R2/hPCFT4	R2(VC)	KB	KB (+FA)	IGROV1	IGROV1 (+FA)
3a	101.0(16.6)	273.5(49.1)	0.31 (0.14)	>1000	3.34 (0.26)	288(12)	0.26(0.03)	>1000	0.55(0.10)	>1000
3b	>1000	>1000	1.82(0.28)	>1000	43.4(4.1)	>1000	0.55(0.10)	>1000	0.97(0.12)	>1000
4	>1000	>1000	>1000	>1000	>1000	>1000	171(36)	>1000	ND	ND
5	>1000	>1000	>1000	>1000	>1000	>1000	267(33)	>1000	ND	ND
6	>1000	>1000	147(53)	>1000	>1000	>1000	35.3(4.4)	>1000	102.9(25.9)	>1000
7	>1000	>1000	2.54(0.52)	>1000	41.54(13.09)	>1000	0.17(0.02)	>1000	0.48(0.08)	>1000
8	>1000	>1000	2.60(0.59)	>1000	63.82(16.23)	>1000	0.27(0.07)	>1000	1.4(0.5)	>1000
9	>1000	>1000	>1000	>1000	>1000	>1000	>1000	>1000	ND	ND
10	>1000	>1000	>1000	>1000	>1000	>1000	>1000	>1000	ND	ND
11	>1000	>1000	>1000	>1000	>1000	>1000	>1000	>1000	ND	ND
12	>1000	>1000	13.48(2.42)	>1000	>1000	>1000	>1000	>1000	>1000	>1000
13	>1000	>1000	8.26 (1.86)	>1000	>1000	>1000	>1000	>1000	>1000	>1000
20	>1000	>1000	12.07(5.02)	>1000	>1000	>1000	>1000	>1000	>1000	>1000
MTX	12(1.1)	216(8.7)	114(31)	461(62)	120.5(16.8)	>1000	6.0(0.6)	20(2.4)	21(3.4)	22(2.1)
PMX	138(13)	894(93)	42(9)	388(68)	13.2(2.4)	974.0(18.1)	68(12)	327(103)	102(25)	200(18)
RTX	6.3(1.3)	>1000	15(5)	>1000	99.5(11.4)	>1000	5.9(2.2)	22(5)	12.6(3.3)	20(4.3)
LMTX	12(2.3)	>1000	12(8)	188(41)	38.0(5.3)	>1000	1.2(0.6)	31(7)	3.1(0.9)	16(6)

[a]Growth inhibition assays were performed for CHO sublines engineered to express RFC (PC43-10), FRα (RT16), or PCFT (R2/hPCFT4), for comparison with transporter-null [R2, R2(VC)] CHO cells, and for the KB and IGROV1 tumor sublines (express RFC, FRα, and PCFT), as described in the Experimental Section. For the FR experiments, growth inhibition assays were performed in the presence and the absence of 200 nM folic acid (FA). The data shown are mean values from 2−10 experiments (plus/minus SEM in parentheses). Results are presented as IC_{50} (in nM), corresponding to the concentration that inhibit growth by 50% relative to cells incubated without drug. Data for MTX, PMX, RTX, and LMTX were previously published.[10−14]. ND: not determined

both compounds **7** and **8** (but not conformationally rigid **13** and **20**) inhibited proliferation of R2/hPCFT4 cells (IC_{50}s of 41.5 and 63.8 nM for **7** and **8**, respectively), essentially equivalent to compound **3b** (IC_{50} of 43.4 nM). This establishes cellular uptake of compounds **7** and **8** by PCFT. Drug sensitivities for **7** and **8** with R2/hPCFT4 cells exceeded those for MTX and RTX and were comparable to those for LMTX. However, **7** and **8** were less potent than PMX (~3- and ~5-fold, respectively) and **3a** (~12- and ~19-fold, respectively). None of the 6-substituted pyrrolo[2,3-*d*]pyrimidine regioisomers (**3b**, **4**−**13**, and **20**) had any impact on proliferation of R2 or R2(VC) cells.

For FRα-expressing RT16 cells, compounds **4**, **5**, **10**, and **11** were all inert at drug concentrations up to 1000 nM. Compounds **6**, **7**, **8**, **12**, **13**, and **20**, like **3b**, all showed some level of antiproliferative activity toward RT16 cells. The active drugs followed an order of potency, **7** ~ **8** ~ **3b** > **12** ~ **13** > **20** ≫ **6**. FR-mediated growth inhibitions for the most active analogues (i.e., **3b**, **7**, and **8**) exceeded those for standard antifolates (Table 1), and for all the active analogues, inhibitions were abolished with 100-fold excess folic acid.

KB and IGROV1 human tumor cells express all three transport systems[7] and in these models, **7** and **8** were the most potent drugs in our series (Table 1). Inhibitory activities for **7** and **8** were similar to those for **3a** and **3b** in both KB and IGROV1 cells. In KB cells, compounds **4**, **5**, and **6** were all substantially less active than **7** and **8**, in order of decreasing potency, **6** ≫ **5** ~ **4**. For the active analogues, growth inhibition was again reversed by excess folic acid, establishing that, like compound **3b**, FRα was the major mechanism of uptake in these cells despite the presence of RFC and PCFT. Thus, for the **7** and **8** regioisomers of **3b**, we confirmed our hypothesis that by varying the distance between the bicyclic scaffold and the L-glutamate, we preserved both the absolute selectivity of **3b** and the high antiproliferative potencies of **3a** and **3b**.

Interestingly, none of the acetylenic compounds (**9**−**13** and **20**) were inhibitory toward FRα-expressing human KB cells, in striking contrast to the results with RT16 CHO cells with compounds **12**, **13**, and **20**. This suggests that for **12**, **13**, and **20**, there must be differences in cellular metabolism, drug binding to intracellular targets, and/or substrate activity for folylpolyglutamate synthetase between the human and hamster cells. When several of these analogues (**3b**, **6**, **12**, **13**, and **20**, compared to **7** and **8**) were tested in IGROV1 cells, results analogous to those with KB cells were obtained (Table 1).

Additional experiments used colony-forming assays with KB tumor cells continuously exposed to **3b**, **7**, or **8** for up to 14 days, after which colonies were stained with 1% methylene blue and counted. Compounds **7** and **8** inhibited KB cell colony formation (Supporting Information, Figure 1S) with IC_{50}s (0.39 and 0.16 nM, respectively) similar to that for compound **3b** (IC_{50} = 0.20 nM) and substantially lower than that for MTX (IC_{50} = 8.5 nM).

These results establish that (i) none of the regioisomers **3b**, **4**−**13**, and **20** are RFC substrates. (ii) For the saturated bridge analogues (**3b**, **4**−**8**), a 1,3-relationship between the carbon bridge domain and the L-glutamate moiety is an important determinant of transport substrate activity with FRα or PCFT. (iii) Compounds **7** and **8**, like **3b**, were substantially less inhibitory toward PCFT-expressing cells than compound **3a**. However, this difference was much reduced in human tumor cells for which FRα was the primary mode of drug delivery. The results with compounds **4**, **5**, and **6** and FRα-expressing cells suggest that decreasing distance between the bicyclic ring and the L-glutamate beyond a point has adverse effects on drug activity, analogous to those resulting from decreasing bridge

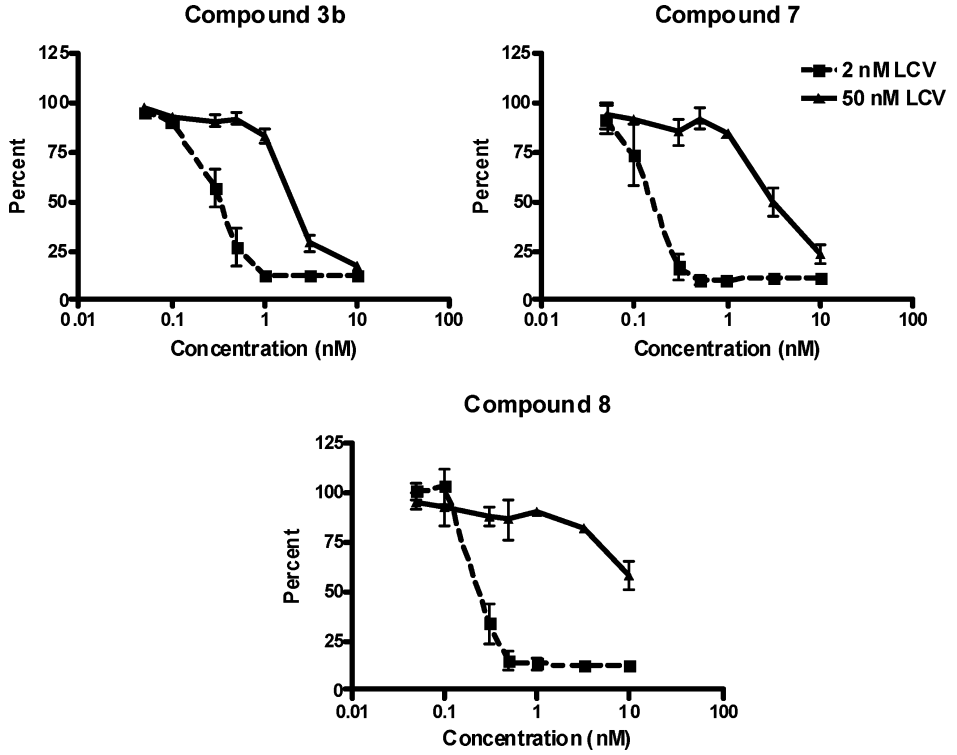

Figure 3. Growth inhibition of KB cells by the 6-substituted pyrrolo[2,3-*d*]pyrimidine thienoyl regioisomers **3b**, **7**, and **8** in the presence of physiologic concentrations of reduced folate. Cell proliferation inhibition was measured over a range of concentrations of the antifolates in complete folate-free RPMI1640 in the presence of LCV at 2 and 50 nM. Cell densities were measured as in the Experimental Section with a fluorescence dye and a fluorescence plate reader. Results were normalized to cell density in the absence of drug. Results shown are average values plus/minus ranges for duplicate experiments.

lengths to less than three atoms. (iv) None of the conformationally restricted acetylenic analogues (**9**−**13** and **20**) were substrates for PCFT. (v) For this series, the [1,3] acetylenic analogues (**12**, **13**, and **20**) are substrates for FRα, although other factors unrelated to membrane transport seem likely to account for the marked differences in their antiproliferative activities between the human and hamster sublines.

Impact of Elevated Leucovorin and Nucleosides on Antitumor Activities of Compounds 7 and 8. Since our proliferation assays with FR-expressing cells routinely use limiting (2 nM) concentrations of extracellular leucovorin [(6*R*,*S*)5-formyl tetrahydrofolate, a chemically stable reduced folate] (LCV), additional experiments were performed with KB cells to assess the impact of elevated (50 nM) LCV [for which the active (6*S*) stereoisomer approximates the concentration of 5-methyl tetrahydrofolate in serum] on the growth inhibitory effects of the most potent analogues (compounds **7** and **8**) of our series compared to compound **3b** (Figure 3). In KB cells, the impact of 50 nM LCV was uneven and ranged from ∼7-fold for **3b** to ∼20-fold for **7** and >38-fold for **8**. For the data in Figure 3, IC_{50} values in the presence of 50 nM LCV were 2.2 nM for **3b**, 3.4 nM for **7**, and >20 nM for **8**. Thus, both compounds **3b** and **7** maintained substantial antitumor potencies even in the presence of elevated physiologic levels of reduced folate.

As previously reported for **3b**,[12] growth inhibitory effects of **7** and **8** toward KB (Figure 4) and IGROV1 cells (not shown) were completely reversed when drug exposures were performed in the presence of adenosine (60 μM) but not thymidine (10 μM). This established that the effects of **7** and **8** on cell proliferation were the consequence of inhibiting the de novo purine nucleotide biosynthetic pathway. For both **7** and **8**, 5-amino-4-imidazolecarboxamide (AICA) (320 μM) was also protective. Since AICA is metabolized to AICA ribonucleotide (AICAR), the substrate for AICAR formyltransferase (AICARFTase, the second folate-dependent reaction after GARFTase),[10,19] **7** and **8** must derive their growth inhibitory effects by inhibiting GARFTase. This was further tested below.

Cellular Pharmacology of Cytotoxic 6-Substituted Pyrrolo[2,3-*d*]pyrimidine Thienoyl Regioisomers. Results of our cell proliferation assays in engineered CHO and human tumor cells suggested that **7** and **8** are bona fide transport substrates for FRα and PCFT. From results of nucleoside and AICA protection studies, **7** and **8**, like **3b**, following internalization, inhibit de novo purine nucleotide biosynthesis apparently at the level of GARFTase. Interestingly, whereas the acetylenic bridge analogues **12**, **13**, and **20** inhibited proliferation of FRα-expressing RT16 CHO cells, these compounds were *inactive* toward human tumor cells.

Using inhibition of human tumor cell proliferation as a primary metric, we selected compounds **3b** and **4**−**8** for testing FRα binding, reflected in competitive inhibition of [^{3}H]folic acid binding to FRα in RT16 CHO cells. For these experiments, RT16 cells were washed with acid-buffered saline (pH 3.5), treated (at neutral pH) with 50 nM [^{3}H]folic acid, along with a range of concentrations of the pyrrolo[2,3-*d*]pyrimidines **3b** and **4**−**8**, folic acid, LMTX, PMX, or MTX. After additional washes (neutral pH), cells were solubilized (in 0.5 N NaOH). FRα-bound [^{3}H]folic acid was measured and normalized to cellular protein, and relative inhibitor affinities were calculated as inverse molar ratios of the concentrations of unlabeled ligands which decreased [^{3}H]folic acid binding by 50%.

dx.doi.org/10.1021/jm201688n | *J. Med. Chem.* 2012, 55, 1758−1770

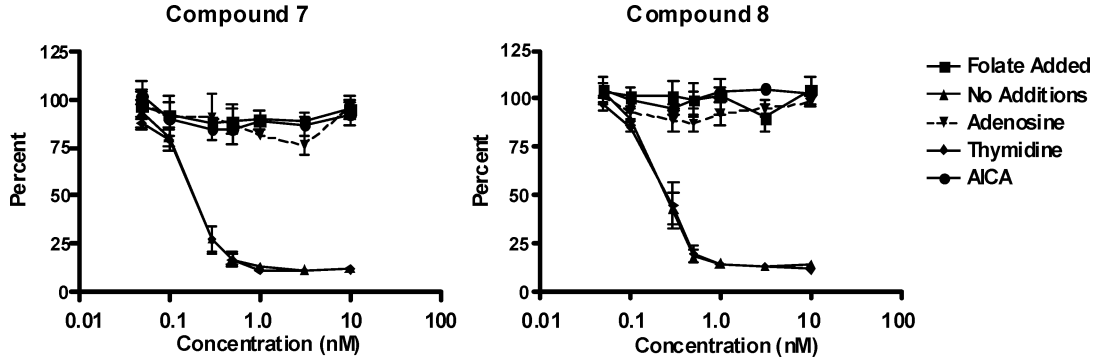

Figure 4. Protection of KB cells from growth inhibition by the 6-substituted pyrrolo[2,3-*d*]pyrimidine thienoyl regioisomers **7** and **8** in the presence of nucleosides and 5-amino-4-imidazolecarboxamide (AICA). Proliferation inhibition was measured for KB cells over a range of concentrations of compounds **7** and **8**, as shown, in complete folate-free RPMI1640 with 2 nM LCV in the absence of other additions (labeled "no additions") or in the presence of 200 nM folic acid (labeled "folate-added"), adenosine (60 μM), thymidine (10 μM), or AICA (320 μM). Cell densities were measured as in the Experimental Section with a fluorescence dye and a fluorescence plate reader. Results were normalized to cell densities in the absence of drug. Results shown are representative data of experiments performed in triplicate. Analogous results were obtained with IGROV1 cells (not shown).

In these experiments, compounds **7** and **8** were all high affinity ligands (relative affinities of $\geq$1) for FRα, essentially equivalent to **3b** and folic acid and substantially better than LMTX (Figure 5). Like MTX, compounds **4**–**6** did not bind to

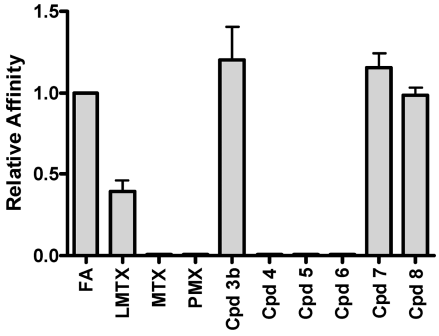

Figure 5. Binding of 6-substituted pyrrolo[2,3-*d*]pyrimidine thienoyl regioisomers (**3b**, **4**–**8**) to FRα. Data are shown for the effects of the unlabeled ligands with FRα-expressing RT16 CHO cells. Relative binding affinities for assorted folate/antifolate substrates were determined over a range of ligand concentrations and were calculated as the inverse molar ratios of unlabeled ligands required to inhibit [^{3}H]folic acid binding by 50%. By definition, the relative affinity of folic acid is 1. Details for the binding assays are provided in the Experimental Section. Results are presented as average values and ranges from two to three experiments. Undefined abbreviations are as follows: FA, folic acid.

FRα in this assay, in spite of detectable (albeit lower) levels of FRα-directed activity in our cell proliferation experiments (with KB cells, Table 1). The detectable antiproliferative activities with **4**, **5**, and **6** in KB cells (but not RT16 CHO cells) likely reflect markedly elevated levels of FRα in this human tumor cell line, as previously reported.[10]

Since compounds **7** and **8** inhibited proliferation of R2/hPCFT4 cells, these analogues were tested as competitive inhibitors of PCFT transport of [^{3}H]MTX in R2/hPCFT4 cells. Experiments were performed at pH 5.5, approximating the pH optimum for PCFT, and at pH 6.8, which is commonly achieved during cell outgrowth.[14] K_i values were calculated over a range of inhibitor concentrations from Dixon plots, and results were compared to those for **3b** and PMX (Table 2). At pH 5.5, K_i values for **3b**, **7**, and **8** were all similar (within a factor of ~2)

Table 2. K_i for PCFT Substrates[a]

	K_i (μM)	
substrate	pH 5.5	pH 6.8
3b	0.23 ± 0.06 (n = 7)	7.23 ± 2.23 (n = 7)
7	0.39 ± 0.10 (n = 4)	28.1 ± 5.3 (n = 4)
8	0.42 ± 0.11 (n = 4)	30.7 ± 8.5 (n = 4)
PMX	0.094 ± 0.006 (n = 8)	2.54 ± 0.31 (n = 8)

[a] K_i values for PCFT substrates were determined by Dixon plots with [^{3}H]MTX as substrate and a range of inhibitor concentrations in R2/hPCFT4 cells. K_i values were calculated from the slopes of the Dixon plots and kinetic constants (K_t and V_{max}) for MTX. Results are presented as mean values ± standard errors from multiple experiments (numbers shown in parentheses).

and approached the K_i for PMX. At pH 6.8, K_i values for PMX and **3b** were likewise similar (~27- and 31-fold higher, respectively, than the values at pH 5.5). In comparison, K_i values for **7** and **8** were further increased at pH 6.8 (~70-fold greater) over the K_i values recorded at pH 5.5.

Collectively, these experiments confirm the high affinity binding for the [1,3] thienoyl regioisomers **3b**, **7**, and **8** to FRα and PCFT, suggested from their potent antiproliferative and cytotoxic effects toward FRα- and PCFT-expressing CHO and human tumor cells. While compounds **7** and **8**, like **3b**, are potent inhibitors of PCFT at pH 5.5, binding of **7** and **8** to PCFT (as reflected in K_i) appears to be more sensitive to pH than for either **3b** or PMX.

Results of nucleoside/AICA protection experiments with KB (Figure 4) and IGROV1 tumor cells (not shown) suggested that GARFTase in the de novo purine nucleotide biosynthetic pathway was the primary intracellular target of **7** and **8**, analogous to **3b**,[12] thus explaining the potent antiproliferative activities of these agents. To confirm GARFTase inhibition with compounds **7** and **8**, we used an in situ GARFTase activity assay in which intact cells were incubated with the antifolate drugs along with [^{14}C]glycine as a radiotracer. In the presence of azaserine, [^{14}C]glycine is incorporated into GAR, accumulating [^{14}C]formyl GAR which can be isolated by ion exchange chromatography, and radioactivity is determined.[10−13,19]

Data are shown in Figure 6 for the effects of compounds **3b**, **7**, and **8** on in situ GARFTase activity in IGROV1 cells, although completely analogous results were obtained with KB

dx.doi.org/10.1021/jm201688n | J. Med. Chem. 2012, 55, 1758−1770

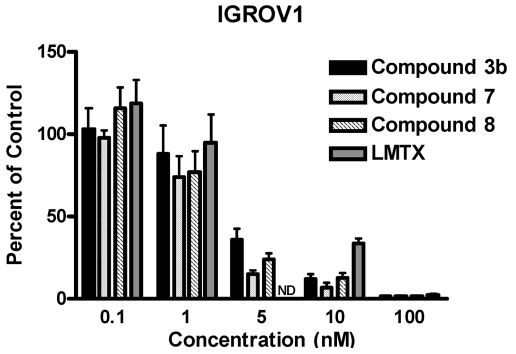

Figure 6. In situ GARFTase inhibition assay. For the in situ assays, incorporation of [^{14}C]glycine into [^{14}C]formyl GAR was measured in IGROV1 tumor cells cultured for 15 h in complete folate-free RPMI plus 2 nM LCV. Details are described in the Experimental Section. Results are presented as a percent of controls treated without drugs for IGROV1 cells treated with nanomolar concentrations of **3b**, **7**, **8**, or LMTX. LMTX was not tested at 5 nM (labeled "ND" for not determined). Results are presented as average values plus/minus ranges. Mean IC_{50} values were calculated as 3.46 nM for **3b**, 1.79 nM for **7**, 2.03 nM for **8**, and 5.77 nM for LMTX.

cells (not shown). In this assay, **3b**, **7**, and **8**, like LMTX, were all potent inhibitors at low nanomolar concentrations.

CONCLUSIONS

A lack of selectivity for folate transporters is a major cause of toxicity and chemotherapy failure with clinically used antifolates. We previously reported potent inhibition of tumor cell proliferation by a classical 2-amino-4-oxo-6-substituted pyrrolo[2,3-*d*]pyrimidine with a thienoyl-for-benzoyl-substituted side chain and a four-carbon bridge (compound **3b**).[7,12] Compound **3b** was selective for transport by FRs and PCFT over RFC and inhibited GARFTase in de novo purine biosynthesis.[7,12] An analogue of this series with a three-carbon bridge (compound **3a**) was even more active, suggesting that the distance between the bicyclic scaffold and L-glutamate could be an important determinant of drug activity, although this may be partly at the expense of absolute transport selectivity.[13] Accordingly, we pursued other approaches for altering this feature, without appreciably impacting drug potency toward PCFT- and FRα-expressing cells while preserving selectivity for transport by non-RFC uptake mechanisms over RFC.

We now describe the synthesis and biological characterization of regioisomers of **3b** (compounds **4**–**8**), differing in positions of thienoyl ring substitution to vary the distance and orientation between the bicyclic scaffold and the L-glutamate. Additional conformationally restricted analogues of **3b** and **4**–**8** (designated **20** and **9**–**13**, respectively) were also studied in which a linear acetylenic linkage was inserted into the bridge region. Of this expanded series, analogues with a saturated bridge and with a [1,3] substitution pattern on the thienoyl ring (compounds **3b**, **7**, and **8**) were the best inhibitors of KB and IGROV1 human tumor cell growth and clonogenicity. This was associated with a potent inhibition of GARFTase in de novo purine nucleotide biosynthesis. Whereas compounds **3b**, **7**, and **8** all showed FRα- and PCFT-mediated effects on cell proliferation, neither **3b** nor compounds **4**–**8** showed activity toward CHO cells expressing only RFC. Further, none of the conformationally restricted linear acetylenic bridge analogues **9**–**13** and **20** inhibited human tumor cell growth, although the [1,3] thiophene-substituted compounds **12**, **13**, and **20** were distinctly (and selectively) inhibitory toward FRα-expressing RT16 CHO cells. This further supports our conclusion that only the [1,3] substituted thiophene is amenable to high affinity FRα binding and cellular uptake and that species differences in intracellular drug metabolism and/or target enzyme binding must account for the lack of activity of these acetylenic analogues with human tumor cells.

Thus, our present and published results establish that the pyrrolo[2,3-*d*]pyrimidine scaffold, along with a thienoyl side chain, is particularly amenable to FR and PCFT transport in the absence of RFC transport and to potent GARFTase inhibition. Our new finding that [1,3] substituted regioisomers of this series are preferred over the [1,2] analogues is consistent with the notion of an optimal distance between the bicyclic ring system and L-glutamate moiety for maximal antiproliferative effects. However, among [1,3] compounds **3b**, **7**, and **8**, or even including **3a**, there was no consistent relationship between relative drug sensitivities toward FRα- and PCFT-expressing cells and these intramolecular distances. Indeed, compounds **7** and **8** showed in vitro potencies that were generally comparable to those for compound **3b** or even **3a**, although this was cell line-dependent. This may reflect differential impacts of extra- and/or intracellular reduced folates on efficacies of the various analogues, combined with cell-specific differences in folate transport (i.e., RFC levels) or metabolism and, for PCFT, differences in relative binding affinities between drugs at pH ~6.8.

Of course, the most distinguishing feature of the three active regioisomers **3b**, **7**, and **8** is their complete lack of RFC-mediated growth inhibition (presumably reflecting their lack of uptake), which is key to their potential therapeutic utility, as this would obviate toxicity to normal susceptible tissues for which drug transport by FRs or PCFT should be nominal. Clearly, the profound selectivity of these novel 6-substituted pyrrolo[2,3-*d*]pyrimidine[1,3]thienoyl antifolates for FRs and PCFT over RFC offers a paradigm for selective tumor targeting, based on established patterns of FR and PCFT expression in human tumors[7] and optimal PCFT membrane transport under acidic conditions characteristic of the solid tumor microenvironment.

EXPERIMENTAL SECTION

All evaporations were carried out in vacuum with a rotary evaporator. Analytical samples were dried in vacuo (0.2 mmHg) in a CHEM-DRY drying apparatus over P_2O_5 at 60 °C. Melting points were determined on a MEL-TEMP II melting point apparatus with FLUKE 51 K/J electronic thermometer and are uncorrected. Nuclear magnetic resonance spectra for proton (^{1}H NMR) were recorded on Bruker Avance II 400 (400 MHz) and 500 (500 MHz) spectrometers. The chemical shift values are expressed in ppm (parts per million) relative to tetramethylsilane as an internal standard: s, singlet; d, doublet; t, triplet; q, quartet; m, multiplet; br, broad singlet. Thin-layer chromatography (TLC) was performed on Whatman Sil G/UV254 silica gel plates with a fluorescent indicator, and the spots were visualized under 254 and 366 nm illumination. Proportions of solvents used for TLC are by volume. Column chromatography was performed on a 230–400 mesh silica gel (Fisher, Somerville, NJ) column. The amount (weight) of silica gel for column chromatography was in the range of 50–100 times the amount (weight) of the crude compounds being separated. Columns were dry-packed unless specified otherwise. Elemental analyses were performed by Atlantic Microlab, Inc., Norcross, GA. Element compositions are within ±0.4% of the calculated values. Fractional moles of water or organic solvents frequently found in some analytical samples of antifolates could not be prevented despite 24–48 h of drying in vacuo and were confirmed where possible by their presence in the ^{1}H NMR spectra. Elemental analysis was used to determine the purities of the final compounds **4**–**13**. All solvents

dx.doi.org/10.1021/jm201688n | J. Med. Chem. 2012, 55, 1758–1770

and chemicals were purchased from Aldrich Chemical Co. and Fisher Scientific and were used as received. Purities of the final compounds **4**–**13** were >95% and were determined by elemental (C, H, N, S) analysis.

General Procedure for the Synthesis of Compounds 15a–e. To a 250 mL round-bottomed flask was added a mixture of bromo-substituted thiophenecarboxylic acid **14a–e** (1.04 g, 5 mmol), *N*-methylmorpholine (909 mg, 9 mmol), 2-chloro-4,6-dimethoxy-1,3,5-triazine (1.58 g, 9 mmol), and anhydrous DMF (20 mL). The mixture was stirred for 1.5 h at room temperature. *N*-Methylmorpholine (909 mg, 9 mmol) and L-glutamic acid diethyl ester hydrochloride (1.8 g, 7.5 mmol) were added to the flask, and the reaction mixture was then stirred at room temperature for 12 h. After evaporation of solvent under reduced pressure, MeOH (20 mL) was added followed by silica gel (2.5 g). The resulting plug was loaded onto a silica gel column (2.5 cm × 12 cm) and eluted with 50% EtOAc in hexane. Fractions with the desired R_f (TLC) were pooled and evaporated to afford **15a–e** as colorless liquid.

(*S*)-2-[(2-Bromothiophene-3-carbonyl)amino]pentanedioic Acid Diethyl Ester (15a). Compound **15a** was prepared using the general method described for the preparation of **15a–e**, from 2-bromo-thiophene-3-carboxylic acid, **14a** (1.04 g, 5 mmol), to give 1.76 g (90%) of **15a** as a colorless liquid. TLC R_f = 0.44 (hexane/EtOAc, 1:1). ^{1}H NMR ($CDCl_3$-d_1): δ 1.24–1.35 (m, 6H, $COOCH_2CH_3$), 2.09–2.56 (m, 4H, β-CH_2, γ-CH_2), 4.10–4.17 (m, 2H, $COOCH_2CH_3$), 4.23–4.29 (m, 2H, $COOCH_2CH_3$), 4.78–4.86 (m, 1H, α-CH), 7.20–7.22 (d, J = 7.2 Hz, 1H, CONH, exch), 7.26–7.27 (d, J = 5.6 Hz, 1H, Ar), 7.36–7.37 (d, J = 5.6 Hz, 1H, Ar).

(*S*)-2-[(3-Bromothiophene-2-carbonyl)amino]pentanedioic Acid Diethyl Ester (15b). Compound **15b** was prepared using the general method described for the preparation of **15a–e**, from 3-bromo-thiophene-2-carboxylic acid, **14b** (1.04 g, 5 mmol), to give 1.8 g (91%) of **15b** as a colorless liquid. TLC R_f = 0.45 (hexane/EtOAc, 1:1). ^{1}H NMR ($CDCl_3$-d_1): δ 1.24–1.36 (m, 6H, $COOCH_2CH_3$), 2.13–2.55 (m, 4H, β-CH_2, γ-CH_2), 4.10–4.16 (m, 2H, $COOCH_2CH_3$), 4.25–4.30 (m, 2H, $COOCH_2CH_3$), 4.83–4.88 (m, 1H, α-CH), 7.07–7.08 (d, J = 5.6 Hz, 1H, Ar), 7.48–7.49 (d, J = 5.6 Hz, 1H, Ar), 7.73–7.75 (d, J = 7.2 Hz, 1H, CONH, exch).

(*S*)-2-[(4-Bromothiophene-3-carbonyl)amino]pentanedioic Acid Diethyl Ester (15c). Compound **15c** was prepared using the general method described for the preparation of **15a–e**, from 4-bromo-thiophene-3-carboxylic acid, **14c** (1.04 g, 5 mmol), to give 1.74 g (89%) of **15c** as a colorless liquid. TLC R_f = 0.45 (hexane/EtOAc, 1:1). ^{1}H NMR ($CDCl_3$-d_1): δ 1.24–1.35 (m, 6H, $COOCH_2CH_3$), 2.07–2.56 (m, 4H, β-CH_2, γ-CH_2), 4.11–4.17 (m, 2H, $COOCH_2CH_3$), 4.23–4.30 (m, 2H, $COOCH_2CH_3$), 4.78–4.87 (m, 1H, α-CH), 7.35–7.36 (d, J = 3.6 Hz, 1H, Ar), 7.36–7.38 (d, J = 7.2 Hz, 1H, CONH, exch), 8.07–8.08 (d, J = 3.6 Hz, 1H, Ar).

(*S*)-2-[(4-Bromothiophene-2-carbonyl)amino]pentanedioic Acid Diethyl Ester (15d). Compound **15d** was prepared using the general method described for the preparation of **15a–e**, from 4-bromo-thiophene-2-carboxylic acid, **14d** (1.04 g, 5 mmol), to give 1.8 g (91%) of **15d** as a colorless liquid. TLC R_f = 0.44 (hexane/EtOAc, 1:1). ^{1}H NMR ($CDCl_3$-d_1): δ 1.25–1.34 (m, 6H, $COOCH_2CH_3$), 2.13–2.51 (m, 4H, β-CH_2, γ-CH_2), 4.14–4.17 (m, 2H, $COOCH_2CH_3$), 4.23–4.28 (m, 2H, $COOCH_2CH_3$), 4.71–4.76 (m, 1H, α-CH), 7.04–7.06 (d, J = 7.2 Hz, 1H, CONH, exch), 7.42–7.43 (d, J = 1.6 Hz, 1H, Ar), 7.16–7.47 (d, J = 1.6 Hz, 1H, Ar).

(*S*)-2-[(5-Bromothiophene-3-carbonyl)amino]pentanedioic Acid Diethyl Ester (15e). Compound **15e** was prepared using the general method described for the preparation of **15a–e**, from 5-bromo-thiophene-3-carboxylic acid, **14e** (1.04 g, 5 mmol), to give 1.76 g (90%) of **15e** as a colorless liquid. TLC R_f = 0.45 (hexane/EtOAc, 1:1). ^{1}H NMR ($CDCl_3$-d_1): δ 1.25–1.34 (m, 6H, $COOCH_2CH_3$), 2.12–2.53 (m, 4H, β-CH_2, γ-CH_2), 4.12–4.18 (m, 2H, $COOCH_2CH_3$), 4.23–4.28 (m, 2H, $COOCH_2CH_3$), 4.70–4.75 (m, 1H, α-CH), 6.96–6.98 (d, J = 7.2 Hz, 1H, CONH, exch), 7.40–7.41 (d, J = 1.6 Hz, 1H, Ar), 7.83–7.84 (d, J = 1.6 Hz, 1H, Ar).

General Procedure for the Synthesis of Compounds 17a–e. To a 250-mL round-bottomed flask, equipped with a magnetic stirrer and gas inlet, was added a mixture of tetrakis(triphenylphosphine)-palladium(0) (277 mg, 0.24 mmol), triethylamine (1.52 g, 15 mmol), **15a–e** (882 mg, 2.25 mmol), and anhydrous DMF (20 mL). To the stirred mixture, under N_2, were added copper(I) iodide (46 mg, 0.24 mmol) and 2-amino-6-but-3-ynyl-3,7-dihydropyrrolo[2,3-*d*]-pyrimidin-4-one, **16** (303 mg, 1.5 mmol). The reaction mixture was stirred at room temperature overnight (17–18 h). Silica gel (0.5 g) was then added, and the solvent was evaporated under reduced pressure. The resulting plug was loaded onto a silica gel column (1.5 cm × 12 cm) and eluted with $CHCl_3$ followed by 3% MeOH in $CHCl_3$ and then 5% MeOH in $CHCl_3$. Fractions with desired R_f (TLC) were pooled and evaporated to afford **17a–e**.

(*S*)-2-({2-[4-(2-Amino-4-oxo-4,7-dihydro-3*H*-pyrrolo[2,3-*d*]-pyrimidin-6-yl)but-1-ynyl]thiophene-3-carbonyl}amino)-pentanedioic Acid Diethyl Ester (17a). Compound **17a** was prepared using the general method described for the preparation of **17a–e**, from **16** (303 mg, 1.5 mmol) and **15a** (882 mg, 2.25 mmol) to give 412 mg (53%) of **17a** as a brown powder. Mp 81–82 °C. TLC R_f = 0.53 ($CHCl_3$/MeOH, 5:1). ^{1}H NMR (DMSO-d_6): δ 1.16–1.22 (m, 6H, $COOCH_2CH_3$), 1.92–2.14 (m, 2H, β-CH_2), 2.43–2.46 (t, J = 8 Hz, 2H, γ-CH_2), 2.80 (m, 4H, CH_2CH_2), 4.01–4.52 (q, J = 7 Hz, 2H, $COOCH_2CH_3$), 4.10–4.16 (m, 2H, $COOCH_2CH_3$), 4.43–4.48 (m, 1H, α-CH), 5.99 (s, 1H, C5-CH), 6.01 (s, 2H, 2-NH_2, exch), 7.35–7.36 (d, J = 5.5 Hz, 1H, Ar), 7.53–7.54 (d, J = 5.5 Hz, 1H, Ar), 8.34–8.36 (d, J = 7.5 Hz, 1H, CONH, exch), 10.16 (s, 1H, 3-NH, exch), 10.88 (s, 1H, 7-NH, exch).

(*S*)-2-({3-[4-(2-Amino-4-oxo-4,7-dihydro-3*H*-pyrrolo[2,3-*d*]-pyrimidin-6-yl)but-1-ynyl]thiophene-2-carbonyl}amino)-pentanedioic Acid Diethyl Ester (17b). Compound **17b** was prepared using the general method described for the preparation of **17a–e**, from **16** (303 mg, 1.5 mmol) and **15b** (882 mg, 2.25 mmol) to give 423 mg (55%) of **17b** as a brown powder. Mp 77–78 °C. TLC R_f = 0.52 ($CHCl_3$/MeOH, 5:1). ^{1}H NMR (DMSO-d_6): δ 1.16–1.22 (m, 6H, $COOCH_2CH_3$), 1.92–2.18 (m, 2H, β-CH_2), 2.39–2.43 (m, 2H, γ-CH_2), 2.84 (m, 4H, CH_2CH_2), 3.99–4.03 (q, J = 7 Hz, 2H, $COOCH_2CH_3$), 4.14–4.18 (q, J = 7 Hz, 2H, $COOCH_2CH_3$), 4.53–4.57 (m, 1H, α-CH), 6.00 (s, 1H, C5-CH), 6.01 (s, 2H, 2-NH_2, exch), 7.16–7.17 (d, J = 5.0 Hz, 1H, Ar), 7.81–7.82 (d, J = 5.0 Hz, 1H, Ar), 8.19–8.20 (d, J = 7.5 Hz, 1H, CONH, exch), 10.16 (s, 1H, 3-NH, exch), 10.91 (s, 1H, 7-NH, exch).

(*S*)-2-({4-[4-(2-Amino-4-oxo-4,7-dihydro-3*H*-pyrrolo[2,3-*d*]-pyrimidin-6-yl)but-1-ynyl]thiophene-3-carbonyl}amino)-pentanedioic Acid Diethyl Ester (17c). Compound **17c** was prepared using the general method described for the preparation of **17a–e**, from **16** (303 mg, 1.5 mmol) and **15c** (882 mg, 2.25 mmol) to give 433 mg (56%) of **17c** as a brown powder. Mp 80–81 °C. TLC R_f = 0.53 ($CHCl_3$/MeOH, 5:1). ^{1}H NMR (DMSO-d_6): δ 1.16–1.22 (m, 6H, $COOCH_2CH_3$), 1.92–2.14 (m, 2H, β-CH_2), 2.42–2.46 (m, 2H, γ-CH_2), 2.69–2.78 (m, 4H, CH_2CH_2), 4.01–4.05 (q, J = 7 Hz, 2H, $COOCH_2CH_3$), 4.11–4.16 (m, 2H, $COOCH_2CH_3$), 4.45–4.50 (m, 1H, α-CH), 5.99 (s, 1H, C5-CH), 6.00 (s, 2H, 2-NH_2, exch), 7.16–7.17 (d, J = 3.5 Hz, 1H, Ar), 8.08–8.09 (d, J = 3.5 Hz, 1H, Ar), 8.40–8.41 (d, J = 7.5 Hz, 1H, CONH, exch), 10.16 (s, 1H, 3-NH, exch), 10.88 (s, 1H, 7-NH, exch).

(*S*)-2-({4-[4-(2-Amino-4-oxo-4,7-dihydro-3*H*-pyrrolo[2,3-*d*]-pyrimidin-6-yl)but-1-ynyl]thiophene-2-carbonyl}amino)-pentanedioic Acid Diethyl Ester (17d). Compound **17d** was prepared using the general method described for the preparation of **17a–e**, from **16** (303 mg, 1.5 mmol) and **15d** (882 mg, 2.25 mmol) to give 406 mg (53%) of **17d** as a brown powder. Mp 79–80 °C. TLC R_f = 0.53 ($CHCl_3$/MeOH, 5:1). ^{1}H NMR (DMSO-d_6): δ 1.16–1.22 (m, 6H, $COOCH_2CH_3$), 1.92–2.12 (m, 2H, β-CH_2), 2.42–2.45 (t, J = 7.5 Hz, 2H, γ-CH_2), 2.71–2.78 (m, 4H, CH_2CH_2), 4.03–4.07 (q, J = 7 Hz, 2H, $COOCH_2CH_3$), 4.09–4.13 (q, J = 6.5 Hz, 2H, $COOCH_2CH_3$), 4.36–4.40 (m, 1H, α-CH), 6.00 (s, 1H, C5-CH), 6.02 (s, 2H, 2-NH_2, exch), 7.87–7.88 (m, 2H, Ar), 8.76–8.77 (d, J = 7.5 Hz, 1H, CONH, exch), 10.17 (s, 1H, 3-NH, exch), 10.90 (s, 1H, 7-NH, exch).

(*S*)-2-({5-[4-(2-Amino-4-oxo-4,7-dihydro-3*H*-pyrrolo[2,3-*d*]-pyrimidin-6-yl)but-1-ynyl]thiophene-3-carbonyl}amino)-pentanedioic Acid Diethyl Ester (17e). Compound **17e** was

prepared using the general method described for the preparation of **17a−e**, from **16** (303 mg, 1.5 mmol) and **15e** (882 mg, 2.25 mmol) to give 387 mg (50%) of **17e** as a brown powder. Mp 81−82 °C. TLC R_f = 0.53 ($CHCl_3$/MeOH, 5:1). ^{1}H NMR (DMSO-d_6): δ 1.16−1.22 (m, 6H, $COOCH_2CH_3$), 1.92−2.12 (m, 2H, β-CH_2), 2.41−2.44 (t, J = 7.5 Hz, 2H, γ-CH_2), 2.78 (m, 4H, CH_2CH_2), 4.03−4.07 (q, J = 7 Hz, 2H, $COOCH_2CH_3$), 4.09−4.13 (m, 2H, $COOCH_2CH_3$), 4.36−4.41 (m, 1H, α-CH), 6.00 (s, 1H, C5-CH), 6.01 (s, 2H, 2-NH_2, exch), 7.58−7.59 (d, J = 1.5 Hz, 1H, Ar), 8.12−8.13 (d, J = 1.5 Hz, 1H, Ar), 8.56−8.58 (d, J = 7.5 Hz, 1H, CONH, exch), 10.16 (s, 1H, 3-NH, exch), 10.88 (s, 1H, 7-NH, exch).

General Procedure for the Synthesis of Compounds 18a−e. To a Parr hydrogenation flask was added **17a−e** (200 mg, 0.39 mmol), 10% palladium on activated carbon (100 mg), and MeOH (50 mL). Hydrogenation was carried out at 55 psi of H_2 for 4 h. The reaction mixture was filtered through Celite, washed with MeOH (100 mL), and concentrated under reduced pressure to give **18a−e**.

(*S*)-2-({2-[4-(2-Amino-4-oxo-4,7-dihydro-3*H*-pyrrolo[2,3-*d*]-pyrimidin-6-yl)butyl]thiophene-3-carbonyl}amino)pentanedioic Acid Diethyl Ester (18a). Compound **18a** was prepared using the general method described for the preparation of **18a−e**, from **17a** (200 mg, 0.39 mmol) to give 191 mg (95%) of **18a** as a light yellow powder. Mp 81−82 °C. TLC R_f = 0.54 ($CHCl_3$/MeOH, 5:1). ^{1}H NMR (DMSO-d_6): δ 1.15−1.17 (m, 6H, $COOCH_2CH_3$), 1.61 (m, 4H, CH_2CH_2), 1.91−2.12 (m, 2H, β-CH_2), 2.41−2.44 (t, J = 7.0 Hz, 2H, γ-CH_2), 2.51−2.53 (m, 4H, CH_2CH_2), 4.03−4.07 (q, J = 7 Hz, 2H, $COOCH_2CH_3$), 4.08−4.13 (m, 2H, $COOCH_2CH_3$), 4.35−4.40 (m, 1H, α-CH), 5.96 (s, 3H, C5-CH, 2-NH_2, exch), 7.35 (s, 2H, Ar), 8.40−8.42 (d, J = 7.5 Hz, 1H, CONH, exch), 10.99 (s, 1H, 3-NH, exch), 11.35 (s, 1H, 7-NH, exch).

(*S*)-2-({3-[4-(2-Amino-4-oxo-4,7-dihydro-3*H*-pyrrolo[2,3-*d*]-pyrimidin-6-yl)butyl]thiophene-2-carbonyl}amino)pentanedioic Acid Diethyl Ester (18b). Compound **18b** was prepared using the general method described for the preparation of **18a−e**, from **17b** (200 mg, 0.39 mmol) to give 187 mg (93%) of **18b** as a light yellow powder. Mp 80−81 °C. TLC R_f = 0.53 ($CHCl_3$/MeOH, 5:1). ^{1}H NMR (DMSO-d_6): δ 1.15−1.20 (m, 6H, $COOCH_2CH_3$), 1.57 (m, 4H, CH_2CH_2), 1.93−2.12 (m, 2H, β-CH_2), 2.40−2.43 (t, J = 8.0 Hz, 2H, γ-CH_2), 2.51 (m, 2H, CH_2), 2.87 (m, 2H, CH_2), 4.03−4.07 (q, J = 7.0 Hz, 2H, $COOCH_2CH_3$), 4.08−4.14 (m, 2H, $COOCH_2CH_3$), 4.34−4.39 (m, 1H, α-CH), 5.96 (m, 3H, C5-CH, 2-NH_2, exch), 7.02−7.03 (d, J = 5.0 Hz, 1H, Ar), 7.59−7.60 (d, J = 5.0 Hz, 1H, Ar), 8.39−8.40 (d, J = 7.5 Hz, 1H, CONH, exch), 11.09 (s, 1H, 3-NH, exch), 11.41 (s, 1H, 7-NH, exch).

(*S*)-2-({4-[4-(2-Amino-4-oxo-4,7-dihydro-3*H*-pyrrolo[2,3-*d*]-pyrimidin-6-yl)butyl]thiophene-3-carbonyl}amino)pentanedioic Acid Diethyl Ester (18c). Compound **18c** was prepared using the general method described for the preparation of **18a−e**, from **17c** (200 mg, 0.39 mmol) to give 193 mg (96%) of **18c** as a light yellow powder. Mp 79−80 °C. TLC R_f = 0.54 ($CHCl_3$/MeOH, 5:1). ^{1}H NMR (DMSO-d_6): δ 1.17−1.18 (m, 6H, $COOCH_2CH_3$), 1.56 (m, 4H, CH_2CH_2), 1.91−2.11 (m, 2H, β-CH_2), 2.43−2.46 (t, J = 7.5 Hz, 2H, γ-CH_2), 2.46−2.49 (m, 2H, CH_2), 2.75−2.77 (m, 2H, CH_2), 4.03−4.08 (q, J = 7.0 Hz, 2H, $COOCH_2CH_3$), 4.08−4.13 (m, 2H, $COOCH_2CH_3$), 4.35−4.39 (m, 1H, α-CH), 5.83 (s, 1H, C5-CH), 5.98 (s, 2H, 2-NH_2, exch), 7.20−7.21 (d, J = 3.5 Hz, 1H, Ar), 7.92−7.93 (d, J = 3.5 Hz, 1H, Ar), 8.53−8.54 (d, J = 7.5 Hz, 1H, CONH, exch), 10.13 (s, 1H, 3-NH, exch), 10.78 (s, 1H, 7-NH, exch).

(*S*)-2-({4-[4-(2-Amino-4-oxo-4,7-dihydro-3*H*-pyrrolo[2,3-*d*]-pyrimidin-6-yl)butyl]thiophene-2-carbonyl}amino)pentanedioic Acid Diethyl Ester (18d). Compound **18d** was prepared using the general method described for the preparation of **18a−e**, from **17d** (200 mg, 0.39 mmol) to give 185 mg (92%) of **18d** as a light yellow powder. Mp 81−82 °C. TLC R_f = 0.55 ($CHCl_3$/MeOH, 5:1). ^{1}H NMR (DMSO-d_6): δ 1.17−1.19 (m, 6H, $COOCH_2CH_3$), 1.62 (m, 4H, CH_2CH_2), 1.95−2.12 (m, 2H, β-CH_2), 2.41−2.45 (t, J = 7.5 Hz, 2H, γ-CH_2), 2.54−2.62 (m, 4H, CH_2CH_2), 4.03−4.07 (q, J = 7.0 Hz, 2H, $COOCH_2CH_3$), 4.09−4.13 (m, 2H, $COOCH_2CH_3$), 4.36−4.40 (m, 1H, α-CH), 5.99 (s, 3H, C5-CH, 2-NH_2, exch), 7.41 (s, 1H, Ar), 7.76 (s, 1H, Ar), 8.67−8.68 (d, J = 7.5 Hz, 1H, CONH, exch), 11.00 (s, 1H, 3-NH, exch), 11.39 (s, 1H, 7-NH, exch).

(*S*)-2-({5-[4-(2-Amino-4-oxo-4,7-dihydro-3*H*-pyrrolo[2,3-*d*]-pyrimidin-6-yl)butyl]thiophene-3-carbonyl}amino)pentanedioic Acid Diethyl Ester (18e). Compound **18e** was prepared using the general method described for the preparation of **18a−e**, from **17e** (200 mg, 0.39 mmol) to give 183 mg (91%) of **18e** as a light yellow powder. Mp 82−83 °C. TLC R_f = 0.54 ($CHCl_3$/MeOH, 5:1). ^{1}H NMR (DMSO-d_6): δ 1.15−1.18 (m, 6H, $COOCH_2CH_3$), 1.64 (m, 4H, CH_2CH_2), 1.93−2.12 (m, 2H, β-CH_2), 2.41−2.44 (t, J = 7.5 Hz, 2H, γ-CH_2), 2.55 (m, 2H, CH_2), 2.81 (m, 2H, CH_2), 4.03−4.07 (q, J = 7.0 Hz, 2H, $COOCH_2CH_3$), 4.08−4.12 (q, J = 7.0 Hz, 2H, $COOCH_2CH_3$), 4.36−4.40 (m, 1H, α-CH), 5.96 (s, 3H, C5-CH, 2-NH_2, exch), 7.26 (s, 1H, Ar), 7.98 (s, 1H, Ar), 8.46−8.48 (d, J = 8.0 Hz, 1H, CONH, exch), 10.76 (s, 1H, 3-NH, exch), 11.22 (s, 1H, 7-NH, exch).

General Procedure for the Synthesis of Compounds 4−13. To a solution of **18a−e** (100 mg, 0.19 mmol) or **17a−e** (100 mg, 0.19 mmol) in 10 mL of MeOH/$CHCl_3$ (1:1) or MeOH/CH_2Cl_2 (1:1) was added 1 N NaOH (5 mL), and the mixture was stirred under N_2 at room temperature for 16 h. TLC showed the disappearance of the starting material and one major spot at the origin. The reaction mixture was evaporated to dryness under reduced pressure. The residue was dissolved in water (10 mL). The resulting solution was cooled in an ice bath, and the pH was adjusted to 3−4 with dropwise addition of 1 N HCl. The resulting suspension was frozen in a dry ice−acetone bath, thawed to 4−5 °C in the refrigerator, and filtered. The residue was washed with a small amount of cold water and dried in vacuum using P_2O_5 to afford **4−13**.

(*S*)-2-({2-[4-(2-Amino-4-oxo-4,7-dihydro-3*H*-pyrrolo[2,3-*d*]-pyrimidin-6-yl)butyl]thiophene-3-carbonyl}amino)pentanedioic Acid (4). Compound **4** was prepared using the general method described for the preparation of **4−13**, from **15a** (100 mg, 0.19 mmol) to give 83 mg (95%) of **4** as a light yellow powder. Mp 176−177 °C. ^{1}H NMR (DMSO-d_6): δ 1.61 (m, 4H, CH_2CH_2), 1.87−2.10 (m, 2H, β-CH_2), 2.34−2.37 (t, J = 7.5 Hz, 2H, γ-CH_2), 2.47 (m, 2H, CH_2), 3.09−3.11 (m, 2H, CH_2), 4.32−4.37 (m, 1H, α-CH), 5.86 (s, 1H, C5-CH), 5.98 (s, 2H, 2-NH_2, exch), 7.33−7.34 (d, J = 5.0 Hz, 1H, Ar), 7.35−7.36 (d, J = 5.0 Hz, 1H, Ar), 8.28−8.29 (d, J = 7.5 Hz, 1H, CONH, exch), 10.16 (s, 1H, 3-NH, exch), 10.80 (s, 1H, 7-NH, exch), 12.36 (br, 2H, COOH, exch). Anal. ($C_{20}H_{23}N_5O_6S\cdot1.85H_2O$) C, H, N, S.

(*S*)-2-({3-[4-(2-Amino-4-oxo-4,7-dihydro-3*H*-pyrrolo[2,3-*d*]-pyrimidin-6-yl)butyl]thiophene-2-carbonyl}amino)pentanedioic Acid (5). Compound **5** was prepared using the general method described for the preparation of **4−13**, from **18b** (100 mg, 0.19 mmol) to give 83 mg (95%) of **5** as a light yellow powder. Mp 159−160 °C. ^{1}H NMR (DMSO-d_6): δ 1.56 (m, 4H, CH_2CH_2), 1.88−2.11 (m, 2H, β-CH_2), 2.33−2.36 (t, J = 7.5 Hz, 2H, γ-CH_2), 2.48 (m, 2H, CH_2), 2.86−2.88 (m, 2H, CH_2), 4.31−4.36 (m, 1H, α-CH), 5.85 (s, 1H, C5-CH), 5.98 (s, 2H, 2-NH_2, exch), 7.01−7.02 (d, J = 5.0 Hz, 1H, Ar), 7.58−7.59 (d, J = 5.0 Hz, 1H, Ar), 8.24−8.26 (d, J = 7.5 Hz, 1H, CONH, exch), 10.16 (s, 1H, 3-NH, exch), 10.79 (s, 1H, 7-NH, exch), 12.38 (br, 2H, COOH, exch). Anal. ($C_{20}H_{23}N_5O_6S\cdot1.0H_2O$) C, H, N, S.

(*S*)-2-({4-[4-(2-Amino-4-oxo-4,7-dihydro-3*H*-pyrrolo[2,3-*d*]-pyrimidin-6-yl)butyl]thiophene-3-carbonyl}amino)pentanedioic Acid (6). Compound **6** was prepared using the general method described for the preparation of **4−13**, from **18c** (100 mg, 0.19 mmol) to give 83 mg (95%) of **6** as a light yellow powder. Mp 195−196 °C. ^{1}H NMR (DMSO-d_6): δ 1.56 (m, 4H, CH_2CH_2), 1.87−2.10 (m, 2H, β-CH_2), 2.35−2.38 (t, J = 8.0 Hz, 2H, γ-CH_2), 2.47−2.48 (m, 2H, CH_2), 2.75−2.81 (m, 2H, CH_2), 4.32−4.36 (m, 1H, α-CH), 5.85 (s, 1H, C5-CH), 5.96 (s, 2H, 2-NH_2, exch), 7.19−7.20 (d, J = 3.0 Hz, 1H, Ar), 7.92−7.93 (d, J = 3.0 Hz, 1H, Ar), 8.40−8.41 (d, J = 8.0 Hz, 1H, CONH, exch), 10.14 (s, 1H, 3-NH, exch), 10.78 (s, 1H, 7-NH, exch), 12.31 (br, 2H, COOH, exch). Anal. ($C_{20}H_{23}N_5O_6S\cdot0.4CHCl_3$) C, H, N, S.

(*S*)-2-({4-[4-(2-Amino-4-oxo-4,7-dihydro-3*H*-pyrrolo[2,3-*d*]-pyrimidin-6-yl)butyl]thiophene-2-carbonyl}amino)pentanedioic Acid (7). Compound **7** was prepared using the general method described for the preparation of **4−13**, from **18d** (100 mg, 0.19 mmol) to give 83 mg (95%) of **7** as a light yellow powder. Mp 174−175 °C. ^{1}H NMR (DMSO-d_6): δ 1.61 (m, 4H, CH_2CH_2), 1.88−2.11 (m, 2H,

dx.doi.org/10.1021/jm201688n | *J. Med. Chem.* 2012, 55, 1758−1770

β-CH_2), 2.33−2.36 (t, J = 7.5 Hz, 2H, γ-CH_2), 2.56 (m, 4H, CH_2CH_2), 4.32−4.37 (m, 1H, α-CH), 5.88 (s, 1H, C5-CH), 5.96 (s, 2H, 2-NH_2, exch), 7.39 (s, 1H, Ar), 7.75 (s, 1H, Ar), 8.54−8.55 (d, J = 8.0 Hz, 1H, CONH, exch), 10.13 (s, 1H, 3-NH, exch), 10.81 (s, 1H, 7-NH, exch), 12.45 (br, 2H, COOH, exch). Anal. ($C_{20}H_{23}N_5O_6S$·0.31$CHCl_3$) C, H, N, S.

(*S*)-2-({5-[4-(2-Amino-4-oxo-4,7-dihydro-3*H*-pyrrolo[2,3-*d*]-pyrimidin-6-yl)butyl]thiophene-3-carbonyl}amino)pentanedioic Acid (8). Compound **8** was prepared using the general method described for the preparation of **4**−**13**, from **18e** (100 mg, 0.19 mmol) to give 83 mg (95%) of **8** as a light yellow powder. Mp 175−176 °C. ^{1}H NMR (DMSO-d_6): δ 1.64 (m, 4H, CH_2CH_2), 1.87−2.10 (m, 2H, β-CH_2), 2.32−2.35 (t, J = 7.5 Hz, 2H, γ-CH_2), 2.55 (m, 2H, CH_2), 2.80−2.82 (m, 2H, CH_2), 4.33−4.37 (m, 1H, α-CH), 5.88 (s, 1H, C5-CH), 5.96 (s, 2H, 2-NH_2, exch), 7.27 (s, 1H, Ar), 7.96 (s, 1H, Ar), 8.31−8.33 (d, J = 8.0 Hz, 1H, CONH, exch), 10.12 (s, 1H, 3-NH, exch), 10.80 (s, 1H, 7-NH, exch), 12.43 (br, 2H, COOH, exch). Anal. ($C_{20}H_{23}N_5O_6S$·1.5H_2O) C, H, N, S.

(*S*)-2-({2-[4-(2-Amino-4-oxo-4,7-dihydro-3*H*-pyrrolo[2,3-*d*]-pyrimidin-6-yl)but-1-ynyl]thiophene-3-carbonyl}amino)-pentanedioic Acid (9). Compound **9** was prepared using the general method described for the preparation of **4**−**13**, from **17a** (100 mg, 0.19 mmol, dissolved in 10 mL of MeOH/CH_3COOH (9:1)) to give 84 mg (95%) of **9** as a light yellow powder. Mp 196−197 °C. ^{1}H NMR (DMSO-d_6): δ 1.91−2.13 (m, 2H, β-CH_2), 2.34−2.37 (t, J = 7 Hz, 2H, γ-CH_2), 2.81 (m, 4H, CH_2CH_2), 4.41−4.45 (m, 1H, α-CH), 6.01 (s, 3H, C5-CH, 2-NH_2, exch), 7.37−7.38 (d, J = 5.5 Hz, 1H, Ar), 7.53−7.54 (d, J = 5.5 Hz, 1H, Ar), 8.25−8.26 (d, J = 7.5 Hz, 1H, CONH, exch), 10.19 (s, 1H, 3-NH, exch), 10.88 (s, 1H, 7-NH, exch), 12.47 (br, 2H, COOH, exch). Anal. ($C_{20}H_{19}N_5O_6S$·1.0CH_3COOH) C, H, N, S.

(*S*)-2-({3-[4-(2-Amino-4-oxo-4,7-dihydro-3*H*-pyrrolo[2,3-*d*]-pyrimidin-6-yl)but-1-ynyl]thiophene-2-carbonyl}amino)-pentanedioic Acid (10). Compound **10** was prepared using the general method described for the preparation of **4**−**13**, from **17b** (100 mg, 0.19 mmol) to give 83 mg (94%) of **10** as a light yellow powder. Mp 179−180 °C. ^{1}H NMR (DMSO-d_6): δ 1.96−2.18 (m, 2H, β-CH_2), 2.31−2.34 (t, J = 7.5 Hz, 2H, γ-CH_2), 2.84 (m, 4H, CH_2CH_2), 4.41−4.53 (m, 1H, α-CH), 6.01 (s, 3H, C5-CH, 2-NH_2, exch), 7.16−7.17 (d, J = 5.0 Hz, 1H, Ar), 7.80−7.81 (d, J = 5.0 Hz, 1H, Ar), 8.22−8.23 (d, J = 7.5 Hz, 1H, CONH, exch), 10.20 (s, 1H, 3-NH, exch), 10.89 (s, 1H, 7-NH, exch), 12.30 (br, 2H, COOH, exch). Anal. ($C_{20}H_{19}N_5O_6S$·0.3$CHCl_3$) C, H, N, S.

(*S*)-2-({4-[4-(2-Amino-4-oxo-4,7-dihydro-3*H*-pyrrolo[2,3-*d*]-pyrimidin-6-yl)but-1-ynyl]thiophene-3-carbonyl}amino)-pentanedioic Acid (11). Compound **11** was prepared using the general method described for the preparation of **4**−**13**, from **17c** (100 mg, 0.19 mmol) to give 84 mg (95%) of **11** as a light yellow powder. Mp 211−212 °C. ^{1}H NMR (DMSO-d_6): δ 1.92−2.14 (m, 2H, β-CH_2), 2.33−2.37 (t, J = 8.0 Hz, 2H, γ-CH_2), 2.70−2.80 (m, 4H, CH_2CH_2), 4.45−4.50 (m, 1H, α-CH), 6.00 (s, 3H, C5-CH, 2-NH_2, exch), 7.74−7.75 (d, J = 3.0 Hz, 1H, Ar), 8.10−8.11 (d, J = 3.0 Hz, 1H, Ar), 8.30−8.32 (d, J = 8.0 Hz, 1H, CONH, exch), 10.17 (s, 1H, 3-NH, exch), 10.86 (s, 1H, 7-NH, exch), 12.44 (br, 2H, COOH, exch). Anal. ($C_{20}H_{19}N_5O_6S$·0.3$CHCl_3$) C, H, N, S.

(*S*)-2-({4-[4-(2-Amino-4-oxo-4,7-dihydro-3*H*-pyrrolo[2,3-*d*]-pyrimidin-6-yl)but-1-ynyl]thiophene-2-carbonyl}amino)-pentanedioic Acid (12). Compound **12** was prepared using the general method described for the preparation of **4**−**13**, from **17d** (100 mg, 0.19 mmol) to give 85 mg (96%) of **12** as a light yellow powder. Mp 195−196 °C. ^{1}H NMR (DMSO-d_6): δ 1.91−2.11 (m, 2H, β-CH_2), 2.34−2.37 (t, J = 7.5 Hz, 2H, γ-CH_2), 2.71−2.79 (m, 4H, CH_2CH_2), 4.32−4.36 (m, 1H, α-CH), 6.01 (s, 3H, C5-CH, 2-NH_2, exch), 7.86−7.88 (m, 2H, Ar), 8.64−8.65 (d, J = 7.5 Hz, 1H, CONH, exch), 10.16 (s, 1H, 3-NH, exch), 10.88 (s, 1H, 7-NH, exch), 12.46 (br, 2H, COOH, exch). Anal. ($C_{20}H_{19}N_5O_6S$·0.37CH_2Cl_2) C, H, N, S.

(*S*)-2-({5-[4-(2-Amino-4-oxo-4,7-dihydro-3*H*-pyrrolo[2,3-*d*]-pyrimidin-6-yl)but-1-ynyl]thiophene-3-carbonyl}amino)-pentanedioic Acid (13). Compound **13** was prepared using the general method described for the preparation of **4**−**13**, from **17e** (100 mg, 0.19 mmol) to give 84 mg (95%) of **13** as a light yellow powder. Mp 197−198 °C. ^{1}H NMR (DMSO-d_6): δ 1.92−2.14 (m, 2H, β-CH_2), 2.33−2.37 (t, J = 8.0 Hz, 2H, γ-CH_2), 2.70−2.80 (m, 4H, CH_2CH_2), 4.45−4.50 (m, 1H, α-CH), 6.00 (s, 3H, C5-CH, 2-NH_2, exch), 7.74−7.75 (d, J = 3.0 Hz, 1H, Ar), 8.10−8.11 (d, J = 3.0 Hz, 1H, Ar), 8.30−8.32 (d, J = 8.0 Hz, 1H, CONH, exch), 10.17 (s, 1H, 3-NH, exch), 10.86 (s, 1H, 7-NH, exch), 12.44 (br, 2H, COOH, exch). Anal. ($C_{20}H_{19}N_5O_6S$·0.41CH_2Cl_2) C, H, N, S.

(*S*)-2-({5-[4-(2-Amino-4-oxo-4,7-dihydro-3*H*-pyrrolo[2,3-*d*]-pyrimidin-6-yl)but-1-ynyl]thiophene-2-carbonyl}amino)-pentanedioic Acid (20). To a solution of **19** (50 mg, 0.1 mmol) in MeOH (10 mL) was added 1 N NaOH (5 mL), and the mixture was stirred under N_2 at room temperature for 16 h. TLC showed the disappearance of the starting material and one major spot at the origin. The reaction mixture was evaporated to dryness under reduced pressure. The residue was dissolved in water (10 mL). The resulting solution was cooled in an ice bath, and the pH was adjusted to 3−4 with dropwise addition of 1 N HCl. The resulting suspension was frozen in a dry ice−acetone bath, thawed to 4−5 °C in the refrigerator, and filtered. The residue was washed with a small amount of cold water and dried in vacuum using P_2O_5 to afford 43 mg (95%) of **20** as a light yellow powder. Mp 189−190 °C. ^{1}H NMR (DMSO-d_6): δ 1.89−2.05 (m, 2H, β-CH_2), 2.30−2.34 (t, J = 7.6 Hz, 2H, γ-CH_2), 2.76 (m, 4H, CH_2CH_2), 4.33 (m, 1H, α-CH), 5.92 (s, 2H, 2-NH_2, exch), 5.98−5.99 (d, J = 4 Hz, 1H, C5-CH), 7.19−7.20 (d, J = 4 Hz, 1H, Ar), 7.74−7.75 (d, J = 4 Hz, 1H, Ar), 8.69−8.71 (d, J = 8 Hz, 1H, CONH, exch), 10.15 (s, 1H, 3-NH, exch), 10.86 (s, 1H, 7-NH, exch), 12.47 (br, 2H, COOH, exch). HRMS calcd for $C_{20}H_{19}N_5O_6S$ (M + H)$^+$, 458.1134; found, 458.1155.

Reagents for Biological Studies. [3′,5′,7-^{3}H]MTX (20 Ci/mmol), [3′,5′,7,9-^{3}H]folic acid (25 Ci/mmol), and [^{14}C(U)]glycine (87mCi/mmol) were purchased from Moravek Biochemicals (Brea, CA). Unlabeled folic acid was purchased from Sigma Chemical Co. (St. Louis, MO). LCV [(6*R*,*S*)-5-formyl tetrahydrofolate] was provided by the Drug Development Branch, National Cancer Institute, Bethesda, MD. The sources of the classical antifolate drugs were as follows: MTX, Drug Development Branch, National Cancer Institute (Bethesda, MD); RTX [*N*-(5-[*N*-(3,4-dihydro-2-methyl-4-oxyquinazolin-6-ylmethyl)-*N*-methylamino]-2-thienoyl)-L-glutamic acid], AstraZeneca Pharmaceuticals (Maccesfield, Cheshire, England); LMTX (5,10-dideaza-5,6,7,8-tetrahydrofolate) and PMX [*N*-{4-[2-(2-amino-3,4-dihydro-4-oxo-7*H*-pyrrolo[2,3-*d*]pyrimidin-5-yl)ethyl]benzoyl}-L-glutamic acid] (Alimta), Eli Lilly and Co. (Indianapolis, IN). Other chemicals were obtained from commercial sources in the highest available purity.

Cell Lines and Assays of Antitumor Drug Activities. The origin of the engineered CHO sublines including RFC- and FRα-null MTXRIIOua^{R}2-4 (R2), RFC- (pC43-10), PCFT- (R2/PCFT4), or FRα- (RT16) expressing CHO sublines was previously described.[10,11,14,18] Likewise, pDNA3.1 vector control CHO cells (R2/VC) were reported. The CHO cells were cultured in α-minimal essential medium (MEM) supplemented with 10% bovine calf serum (Invitrogen, Carlsbad, CA), 100 units/mL penicillin per 100 μg/mL streptomycin, and 2 mM L-glutamine at 37 °C with 5% CO_2. All the R2 transfected cells [PC43-10, RT16, R2/hPCFT4, R2(VC)] were routinely cultured in α-MEM plus 1.5 mg/mL G418. Prior to the cytotoxicity assays (see below), RT16 cells were cultured in complete folate-free RPMI 1640 (without added folate) for 3 days. R2/hPCFT4 and R2(VC) cells were cultured in complete folate-free RPMI 1640 including dialyzed fetal bovine serum (Invitrogen) and 25 nM LCV plus 1.5 mg/mL G418. KB human nasopharyngeal carcinoma cells were purchased from the American Type Culture Collection (Manassas, VA), whereas IGROV1 ovarian carcinoma cells were a gift of Dr. Manohar Ratnam (University of Toledo, OH). KB and IGROV1 cells were routinely cultured in folate-free RPMI 1640 medium, supplemented with 10% fetal bovine serum, penicillin−streptomycin solution, and 2 mM L-glutamine at 37 °C with 5% CO_2.

For growth inhibition assays, cells (CHO, KB, or IGROV1) were plated in 96-well dishes (~2500−5000 cells/well, total volume of 200 μL of medium) with a range of antifolate concentrations. The medium was RPMI 1640 (contains 2.3 μM folic acid) with 10% dialyzed fetal bovine serum and antibiotics for experiments with R2 and PC43-10 cells. For RT16, KB, and IGROV1 cells, cells were

cultured in folate-free RPMI medium with 10% dialyzed fetal bovine serum and antibiotics supplemented with 2 nM LCV and 2 mM L-glutamine. The requirement for FR-mediated drug uptake in these assays was established in parallel incubations including 200 nM folic acid. For R2/hPCFT4 cells, the medium was folate-free RPMI 1640 (pH 7.2) containing 25 nM LCV, supplemented with 10% dialyzed fetal bovine serum, antibiotics, and L-glutamine. Cells were routinely incubated for up to 96 h, and metabolically active cells (a measure of cell viability) were assayed with CellTiter-blue cell viability assay (Promega, Madison, WI), with fluorescence measured (590 nm emission, 560 nm excitation) using a fluorescence plate reader. Raw data were exported from Softmax Pro software to an Excel spreadsheet for analysis and determinations of IC_{50}s, corresponding to the drug concentrations that result in 50% loss of cell growth.

For some of the in vitro growth inhibition studies, the inhibitory effects of the antifolate inhibitors on de novo thymidylate biosynthesis (i.e., thymidylate synthase) and de novo purine nucleotide biosynthesis (GARFTase and AICARFTase) were tested by co-incubations with thymidine (10 μM) and adenosine (60 μM), respectively. For de novo purine nucleotide biosynthesis, additional protection experiments used AICA (320 μM) to distinguish inhibitory effects at GARFTase from those at AICARFTase.[10−12]

For assays of clonogenicity (colony formation), KB cells (500 cells) were plated in folate-free RPMI1640 medium supplemented with 2 nM LCV, 10% dialyzed fetal bovine serum, penicillin−streptomycin solution, and 2 mM L-glutamine, in the presence of antifolate drugs. The dishes were incubated at 37 °C with 5% CO_2 for 10−14 days. To stain the colonies for counting, the dishes were rinsed with Dulbecco's phosphate-buffered saline (DPBS), 5% trichloroacetic acid, then borate buffer (10 mM, pH 8.8), followed by 30 min of incubation in 1% methylene blue in the borate buffer. The dishes were rinsed with the borate buffer, and colonies were counted for calculating percent colony-forming efficiency normalized to control.

FR Binding Assay. Competitive inhibition of [^{3}H]folic acid binding to FRα with RT16 CHO cells was used to assess relative binding affinities for assorted (anti)folate ligands.[10−12] Briefly, RT16 cells (~1.6 × 10^6) were rinsed twice with DPBS, followed by two washes with an acidic buffer (10 mM sodium acetate, 150 mM NaCl, pH 3.5) to remove FR-bound folates. Cells were washed twice with ice-cold HEPES-buffered saline (20 mM HEPES, 140 mM NaCl, 5 mM KCl, 2 mM $MgCl_2$, 5 mM glucose, pH 7.4) (HBS), then incubated in HBS with [^{3}H]folic acid (50 nM, specific activity 0.5 Ci/mmol) in the presence and absence of unlabeled folic acid or antifolate (over a range of concentrations) for 15 min at 0 °C. The dishes were rinsed three times with ice-cold HBS, after which the cells were solubilized (0.5 N NaOH) and aliquots measured for radioactivity and protein contents. Protein concentrations were measured with Folin phenol reagent.[20] [^{3}H]Folic acid bound to FRα was calculated as pmol/mg protein, and relative binding affinities were calculated as the inverse molar ratios of unlabeled ligands required to inhibit [^{3}H]folic acid binding by 50%. By definition, the relative affinity of folic acid is 1.

Transport Assays. For transport assays, R2/hPCFT4 CHO cells were grown as monolayers and used to seed spinner flasks. For experiments to determine the inhibitions of transport by antifolate substrates, cells were collected from spinners, washed with DPBS, and resuspended in 2 mL of HBS, adjusted to pH 6.8, or 4-morpholinepropanesulfonic acid-buffered saline (20 mM MES, 140 mM NaCl, 5 mM KCl, 2 mM $MgCl_2$, and 5 mM glucose), adjusted to pH 5.5. For determinations of K_i values, cells were incubated with 1 μM [^{3}H]MTX over 2 min at 37 °C in the presence and absence of a range of concentrations of unlabeled antifolates. Controls included a comparable amount of vehicle (DMSO to 0.5%). Uptakes of [^{3}H]MTX were quenched with ice-cold DPBS. Cells were washed with ice-cold DPBS (3×) and solubilized with 0.5 N NaOH. Levels of intracellular radioactivity were expressed as pmol/mg protein, calculated from direct measurements of radioactivity and protein contents of cell homogenates. Protein concentrations were measured with Folin phenol reagent.[20] K_i values were calculated from Dixon plots, and kinetic constants (K_t, V_{max}) for [^{3}H]MTX uptake were calculated from Lineweaver−Burk plots, as previously described.[14]

In Situ GARFT Enzyme Inhibition Assay. Incorporation of [^{14}C]glycine into [^{14}C]formyl GAR, as an in situ measure of endogenous GARFTase activity, was measured as described.[10−12] For these experiments, IGROV1 cells were seeded in 4 mL of complete folate-free RPMI 1640 plus 2 nM LCV in 60 mm dishes at a density of 2 × 10^6 cells per dish. On the next day, the medium was replaced with 2 mL of fresh complete folate-free RPMI 1640 plus 2 nM LCV (without supplementing glutamine). Azaserine (4 μM final concentration) was added in the presence and absence of the antifolate inhibitors. After 30 min, L-glutamine (final concentration, 2 mM) and [^{14}C]glycine (tracer amounts, final specific activity of 0.1 mCi/L) were added. Incubations were at 37 °C for 15 h, at which time cells were washed (one time) with ice-cold folate-free RPMI 1640 plus serum. Cell pellets were treated with 2 mL of 5% trichloroacetic acid at 0 °C. Cell debris was removed by centrifugation (the cell protein contents in the pellets were measured), and the supernatants were extracted twice with 2 mL of ice-cold ether. The aqueous layer was passed through a 1 cm column of AG1x8 (chloride form), 100−200 mesh (Bio-Rad), washed with 10 mL of 0.5 N formic acid and then 10 mL of 4 N formic acid, and finally eluted with 8 mL of 1 N HCl. The eluates were collected and determined for radioactivity. The accumulation of radioactive formyl GAR was calculated as pmol per mg protein over a range of inhibitor concentrations. IC_{50} values were calculated as the concentrations of inhibitors that resulted in a 50% decrease in [^{14}C]formyl GAR synthesis.

■ ASSOCIATED CONTENT

Ⓢ Supporting Information

Colony formation assay data and elemental analysis results. This material is available free of charge via the Internet at http://pubs.acs.org.

■ AUTHOR INFORMATION

Corresponding Author

*For L.H.M.: phone, 313-578-4280; fax, 313-578-4287; e-mail, matherly@kci.wayne.edu. For A.G.: phone, 412-396-6070; fax, 412-396-5593; e-mail, gangjee@duq.edu.

Author Contributions

#These authors contributed equally to this work.

Notes

The authors declare no competing financial interest.

■ ACKNOWLEDGMENTS

This work was supported in part by the National Institutes of Health, National Cancer Institute, Grants CA125153 (A.G.), CA152316 (L.H.M. and A.G.), and CA53535 (L.H.M.); a grant from the Mesothelioma Applied Research Foundation, a pilot grant from the Barbara Ann Karmanos Cancer Institute; and the Duquesne University Adrian Van Kaam Chair in Scholarly Excellence (A.G.). S.K.D. was supported by a Doctoral Research Award from the Canadian Institutes of Health Research (CIHR). S.M.-R. was supported by Grant T32 CA009531 (L.H.M.).

■ ABBREVIATIONS USED

AICA, 5-amino-4-imidazolecarboxamide; AICAR, 5-amino-4-imidazolecarboxamide ribonucleotide; AICARFTase, 5-amino-4-imidazolecarboxamide ribonucleotide formyltransferase; CHO, Chinese hamster ovary; DPBS, Dulbecco's phosphate-buffered saline; FR, folate receptor; GAR, glycinamide ribonucleotide; GARFTase, glycinamide ribonucleotide formyltransferase; HBSS, Hank's balanced salt solution; HEPES, *N*-2-hydroxyethylpiperazine-*N*′-2-ethanesulfonic acid; HBS, *N*-2-hydroxyethylpiperazine-*N*′-2-ethanesulfonic acid buffered saline; IC_{50}, 50% inhibitory concentration; LCV, leucovorin;

LMTX, lometrexol; MEM, minimal essential medium; MTX, methotrexate; PMX, pemetrexed; PCFT, proton-coupled folate transporter; RTX, raltitrexed; RFC, reduced folate carrier

REFERENCES

(1) Matherly, L. H.; Hou, Z.; Deng, Y. Human Reduced Folate Carrier: Translation of Basic Biology to Cancer Etiology and Therapy. *Cancer Metastasis Rev.* **2007**, *26*, 111−128.

(2) Elnakat, H.; Ratnam, M. Distribution, Functionality and Gene Regulation of Folate Receptor Isoforms: Implications in Targeted Therapy. *Adv. Drug Dev.* **2004**, *56*, 1067−1084.

(3) Zhao, R.; Matherly, L. H.; Goldman, I. D. Membrane Transporters and Folate Homeostasis; Intestinal Absorption, Transport into Systemic Compartments and Tissues. *Expert Rev. Mol. Med.* **2009**, *11*, e4.

(4) Zhao, R.; Goldman, I. D. The Molecular Identity and Characterization of a Proton-Coupled Folate Transporter-PCFT; Biological Ramifications and Impact on the Activity of Pemetrexed. *Cancer Metastasis Rev.* **2007**, *26*, 129−139.

(5) Kugel Desmoulin, S.; Wang, Y.; Tait, L.; Hou, Z.; Cherian, C.; Gangjee, A.; Matherly, L. H. Expression Profiling of the Major Folate Facilitative Transporters in Human Tumors and Normal Tissues. *Abstr., Am. Assoc. Cancer Res.* **2010**, *51*, 1103.

(6) Qiu, A.; Min, S. H.; Jansen, M.; Malhotra, U.; Tsai, E.; Cabelof, D. C.; Matherly, L. H.; Zhao, R.; Akabas, M. H.; Goldman, I. D. Rodent Intestinal Folate Transporters (SLC46A1): Secondary Structure, Functional Properties, and Response to Dietary Folate Restriction. *Am. J. Physiol.: Cell Physiol.* **2007**, *293*, C1669−C1678.

(7) Kugel Desmoulin, S.; Wang, L.; Hales, E.; Polin, L.; White, K.; Kushner, J.; Stout, M.; Hou, Z.; Cherian, C.; Gangjee, A.; Matherly, L. H. Therapeutic Targeting of a Novel 6-Substituted Pyrrolo[2,3-*d*]pyrimidine Thienoyl Antifolate to Human Solid Tumors Based on Selective Uptake by the Proton-Coupled Folate Transporter. *Mol. Pharmacol.* **2011**, *80*, 1096−1107.

(8) Gibbs, D. D.; Theti, D. S.; Wood, N.; Green, M.; Raynaud, F.; Valenti, M.; Forster, M. D.; Mitchell, F.; Bavetsias, V.; Henderson, E.; Jackman, A. L. BGC 945, a Novel Tumor-Selective Thymidylate Synthase Inhibitor Targeted to Alpha-Folate Receptor-Overexpressing Tumors. *Cancer Res.* **2005**, *65*, 11721−11728.

(9) Xia, W.; Low, P. S. Folate-Targeted Therapies for Cancer. *J. Med. Chem.* **2010**, *53*, 6811−6824.

(10) Deng, Y.; Wang, Y.; Cherian, C.; Hou, Z.; Buck, S. A.; Matherly, L. H.; Gangjee, A. Synthesis and Discovery of High Affinity Folate Receptor-Specific Glycinamide Ribonucleotide Formyltransferase Inhibitors with Antitumor Activity. *J. Med. Chem.* **2008**, *51*, 5052−5063.

(11) Deng, Y.; Zhou, X.; Kugel Desmoulin, S.; Wu, J.; Cherian, C.; Hou, Z.; Matherly, L. H.; Gangjee, A. Synthesis and Biological Activity of a Novel Series of 6-Substituted Thieno[2,3-*d*]pyrimidine Antifolate Inhibitors of Purine Biosynthesis with Selectivity for High Affinity Folate Receptors over the Reduced Folate Carrier and Proton-Coupled Folate Transporter for Cellular Entry. *J. Med. Chem.* **2009**, *52*, 2940−2951.

(12) Wang, L.; Cherian, C.; Kugel Desmoulin, S.; Polin, L.; Deng, Y.; Wu, J.; Hou, Z.; White, K.; Kushner, J.; Matherly, L. H.; Gangjee, A. Synthesis and Antitumor Activity of a Novel Series of 6-Substituted Pyrrolo[2,3-*d*]pyrimidine Thienoyl Antifolate Inhibitors of Purine Biosynthesis with Selectivity for High Affinity Folate Receptors and the Proton-Coupled Folate Transporter over the Reduced Folate Carrier for Cellular Entry. *J. Med. Chem.* **2010**, *53*, 1306−1318.

(13) Wang, L.; Kugel Desmoulin, S.; Cherian, C.; Polin, L.; White, K.; Kushner, J.; Fulterer, A.; Chang, M.-H.; Mitchell, S.; Stout, M.; Romero, M. F.; Hou, Z.; Matherly, L. H.; Gangjee, A. Synthesis, Biological and Antitumor Activity of a Highly Potent 6-Substituted Pyrrolo[2,3-*d*]pyrimidine Thienoyl Antifolate Inhibitor with Proton-Coupled Folate Transporter and Folate Receptor Selectivity over the Reduced Folate Carrier That Inhibits β-Glycinamide Ribonucleotide Formyltransferase. *J. Med. Chem.* **2011**, *54*, 7150−7064.

(14) Kugel Desmoulin, S.; Wang, Y.; Wu, J.; Stout, M.; Hou, Z.; Fulterer, A.; Chang, M. H.; Romero, M. F.; Cherian, C.; Gangjee, A.; Matherly, L. H. Targeting the Proton-Coupled Folate Transporter for Selective Delivery of 6-Substituted Pyrrolo[2,3-*d*]pyrimidine Antifolate Inhibitors of de Novo Purine Biosynthesis in the Chemotherapy of Solid Tumors. *Mol. Pharmacol.* **2010**, *78*, 577−587.

(15) Helmlinger, G.; Yuan, F.; Dellian, M.; Jain, R. K. Interstitial pH and pO_2 Gradients in Solid Tumors in Vivo: High-Resolution Measurements Reveal a Lack of Correlation. *Nat. Med.* **1997**, *3*, 177−182.

(16) Raghunand, N.; Altbach, M. I.; van Sluis, R.; Baggett, B.; Taylor, C. W.; Bhujwalla, Z. M.; Gillies, R. J. Plasmalemmal pH-Gradients in Drug-Sensitive and Drug-Resistant MCF-7 Human Breast Carcinoma Xenografts Measured by ^{31}P Magnetic Resonance Spectroscopy. *Biochem. Pharmacol.* **1999**, *57*, 309−312.

(17) Wike-Hooley, J. L.; Haveman, J.; Reinhold, H. S. The Relevance of Tumour pH to the Treatment of Malignant Disease. *Radiother. Oncol.* **1984**, *2*, 343−366.

(18) Wong, S. C.; Proefke, S. A.; Bhushan, A.; Matherly, L. H. Isolation of Human cDNAs That Restore Methotrexate Sensitivity and Reduced Folate Carrier Activity in Methotrexate Transport-Defective Chinese Hamster Ovary Cells. *J. Biol. Chem.* **1995**, *270*, 17468−17475.

(19) Beardsley, G. P.; Moroson, B. A.; Taylor, E. C.; Moran, R. G. A New Folate Antimetabolite, 5,10-Dideaza-5,6,7,8-tetrahydrofolate Is a Potent Inhibitor of de Novo Purine Synthesis. *J. Biol. Chem.* **1989**, *264*, 328−333.

(20) Lowry, O. H.; Rosebrough, N. J.; Farr, A. L.; Randall, R. J. Protein Measurement with the Folin Phenol Reagent. *J. Biol. Chem.* **1951**, *193*, 265−275.